Dopamine D1 Receptor Expression Is Bipolar Cell Type-Specific in the Mouse Retina

Pershang Farshi,[1] Bozena Fyk-Kolodziej,[1] David M. Krolewski,[3] Paul D. Walker,[1] and Tomomi Ichinose[1,2]*

[1]Department of Anatomy and Cell Biology, Wayne State University School of Medicine, Detroit, Michigan, USA
[2]Department of Ophthalmology, Wayne State University School of Medicine, Detroit, Michigan, USA
[3]Molecular and Behavioral Neuroscience Institute, University of Michigan Medical School, Ann Arbor, Michigan, USA

ABSTRACT

In the retina, dopamine is a key molecule for daytime vision. Dopamine is released by retinal dopaminergic amacrine cells and transmits signaling either by conventional synaptic or by volume transmission. By means of volume transmission, dopamine modulates all layers of retinal neurons; however, it is not well understood how dopamine modulates visual signaling pathways in bipolar cells. Here we analyzed Drd1a-tdTomato BAC transgenic mice and found that the dopamine D1 receptor (D1R) is expressed in retinal bipolar cells in a type-dependent manner. Strong tdTomato fluorescence was detected in the inner nuclear layer and localized to type 1, 3b, and 4 OFF bipolar cells and type 5-2, XBC, 6, and 7 ON bipolar cells. In contrast, type 2, 3a, 5-1, 9, and rod bipolar cells did not express Drd1a-tdTomato. Other interneurons were also found to express tdTomato including horizontal cells and a subset (25%) of AII amacrine cells. Diverse visual processing pathways, such as color or motion-coded pathways, are thought to be initiated in retinal bipolar cells. Our results indicate that dopamine sculpts bipolar cell performance in a type-dependent manner to facilitate daytime vision. J. Comp. Neurol. 524:2059–2079, 2016.

INDEXING TERMS: BAC transgenic mice; immunohistochemistry; in situ hybridization: RRID: AB_10000347; RRID: AB_2313634; RRID: AB_2079751; RRID: AB_2086774; RRID: AB_2094841; RRID: AB_2314280; RRID: AB_10013483; RRID: AB_94936; RRID: AB_2115181; RRID: AB_2248534; RRID: AB_2314947; RRID: AB_2158332; RRID: AB_397957; RRID: AB_628142; RRID: AB_2261205; RRID: AB_10013783; RRID: AB_2201528

Dopamine is a neurotransmitter that is released in the retina during daylight conditions. The modulatory effect of dopamine has been reported in most types of retinal neurons, which is attributable to dopamine signaling conveyed primarily by volume transmission. Dopamine has been shown to regulate coupling between photoreceptors to facilitate cone functions (Ribelayga et al., 2008; Jin et al., 2015), coupling of horizontal cells to alter the efficacy of retinal inhibitory modulation (Mangel and Dowling, 1985; Dong and McReynolds, 1991; Hampson et al., 1994; Xin and Bloomfield, 1999), and connexin 36 between AII amacrine cells to reduce rod-mediated signaling (Deans et al., 2002; Urschel et al., 2006; Kothmann et al., 2009). In the inner retina, dopamine modulates the activity of ganglion cells (Vaquero et al., 2001; Ogata et al., 2012; Van Hook et al., 2012) and bipolar cells (Maguire and Werblin, 1994; Wellis and Werblin, 1995; Ichinose and Lukasiewicz, 2007). Despite this accrual of knowledge, the location of dopamine receptors to specific retinal neurons has not been fully investigated.

Among the five types of dopamine receptors (D1-like: D1 and D5 receptors; D2-like: D2, D3, and D4 receptors), D1 receptors (D1Rs) are expressed in many neurons of the retinal network, while D2-like receptors are detected in photoreceptors and dopaminergic amacrine cells (Cohen et al., 1992; Veruki and Wässle, 1996; Mora-Ferrer et al., 1999; Stella and Thoreson, 2000;

The first two authors contributed equally to this work.

Grant sponsor: National Institutes of Health (NIH); Grant number: R01 EY020533 (to T.I.); Grant sponsor: Mid-West Eye Bank Fund (to P.D.W.); Grant sponsor: WSU Startup Fund (to T.I.); Grant number: NIH P30EY004068 (Vision Core); Grant sponsor: Research to Prevent Blindness (R.P.B.).

*CORRESPONDENCE TO: Tomomi Ichinose, MD, PhD, Dept. of Anatomy and Cell Biology, Ophthalmology, Wayne State University School of Medicine, 540 E. Canfield, Detroit, MI48201. E-mail: tichinos@med.wayne.edu

Received April 29, 2015; Revised November 16, 2015;
Accepted November 17, 2015.
DOI 10.1002/cne.23932
Published online December 8, 2015 in Wiley Online Library (wileyonlinelibrary.com)

Witkovsky, 2004). Veruki and Wässle (1996) analyzed D1R localization in the rat retina using immunocytochemical methods and reported that the D1R was expressed in bipolar cell types 5, 6, and 8, but not in type 2. Approximately a dozen bipolar cell types have recently been elucidated in many species; however, D1R expression has not been reexamined, possibly due to difficulties associated with D1R immunolabeling in somas (Caille et al., 1996; Deng et al., 2006).

Bipolar cells are the second-order neurons in the retina and are responsible for encoding image signaling into separate neural pathways depending on features such as color or motion (Wässle, 2004). These neural pathways are thought to be formed by distinct bipolar cell types (Ghosh et al., 2004; Pignatelli and Strettoi, 2004; Helmstaedter et al., 2013; Euler et al., 2014). Evidence suggests that three types of dopaminergic amacrine (DA) cells extend their processes into multiple layers of the inner plexiform layer (IPL) where bipolar cell axon terminals are located (Zhang et al., 2007; Contini et al., 2010; Volgyi et al., 2014). DA cells process receive excitatory inputs from ON bipolar cells and also make reciprocal connections that return the signal to ON bipolar cells (Dumitrescu et al., 2009; Contini et al., 2010). While these studies suggest that bipolar cells are in position to be exposed to dopamine transmission, dopamine receptor expression in bipolar cells has not been well characterized, and dopaminergic effects on bipolar cell functions remain to be elucidated.

We used the Drd1a-tdTomato BAC transgenic mouse (line 6) developed for D1R research in the striatum (Ade et al., 2011) to investigate D1R-expressing cells in the retina. We employed bipolar cell type-specific markers (Haverkamp et al., 2005; Wässle et al., 2009) and single-cell dye-injection techniques to characterize D1R expression in each bipolar cell type. tdTomato was expressed throughout cells, including dendrites and axon terminals, allowing us to investigate colocalization with type-specific markers. We found evidence that D1Rs are expressed in a bipolar cell type-specific manner, indicating that dopamine regulates specific neural streams at the bipolar cell level.

MATERIALS AND METHODS

Mice

Animal protocols were approved by the Institutional Animal Care and Use Committee of Wayne State University. Wildtype mice (C57BL/6J) used for in-house heterozygous transgenic mice breeding were obtained from Jackson Laboratories (Bar Harbor, ME), as were Drd1a-tdTomato mice (line 6) (JAX stock number 16204). These mice harbor Drd1a BAC (RP23-47M2), which contains the entire Drd1a gene plus 185 kb of 5′ upstream sequence modified to replace the ATG codon plus 180 bp Drd1a coding sequence with tdTomato cDNA (Shuen et al., 2008). Several transgenic lines were generated from this strategy, including line 6, as reported by Ade et al. (2011). Mice were genotyped using standard polymerase chain reaction (PCR) methods on tail sample DNA using the following primers: Drd1a-tdTomato forward 5′-3′CTTCTGAGGCGGAAAGAACC and Drd1a-tdTomato reverse 5′-3′TTTCTGATTGAGAGCATTCG. A single 750 bp product identified mice that were positive for Drd1a-tdTomato expression. Gus8.4-green fluorescent protein (Gus-GFP) mice were kindly donated by Dr. Margolskee (Huang et al., 1999, 2003). Clomeleon 1 mice (B6. Cg-Tg(Thy1-Clomeleon)1Gjau/J) (Clm1-YFP) were purchased from Jackson Laboratory (JAX stock number 013161). Heterozygous Drd1a-tdTomato and Gus-GFP transgenic mice were maintained by in-house breeding for more than five generations. Colonies of Clm1-YFP mice were also maintained in-house. Double transgenic mice with Drd1a-tdTomato and Gus-GFP or Drd1a-tdTomato and Clm1-YFP were generated to investigate D1R colocalization with types-7 and -9 bipolar cells, respectively.

Retinal preparation

Mice (28–60 days old; male) were euthanized using carbon dioxide and pneumothorax. Eyes were removed and placed in cooled, oxygenated dissecting HEPES-buffered solution containing (in mM): 137 NaCl, 2.5 KCl, 2.5 $CaCl_2$, 1.0 $MgCl_2$, 10 HEPES, 28 glucose, adjusted to pH 7.4 with NaOH. Using a dissecting stereomicroscope, the cornea and lens were quickly removed to obtain the eye-cup. For some experiments, the retina was marked to identify dorsal and ventral sides. The eyecups were fixed using 4% paraformaldehyde in 0.1M phosphate buffer (PB) pH 7.4, for 30 minutes at room temperature. After fixation, retinas were separated from the sclera, rinsed several times in 0.1M PB, and cryoprotected in 30% sucrose overnight at 4°C. The tissue was embedded in Tissue Freezing Medium (Electron Microscopy Sciences, Fort Washington, PA; EMS) and was sectioned vertically at 14–16 μm with a Microm HM 525 cryostat (Thermo Fisher Scientific, Waltham, MA). Cryosections were collected on histo-bond slides (Fisher Scientific). For whole-mount retinal preparation, the retina was isolated from the eye-cup in oxygenated HEPES-buffered solution, and was flattened on filter paper (EMD Millipore, Billerica, MA). Then the tissue was fixed using 4% paraformaldehyde for 30 minutes, washed with 0.1M PB, pH 7.4, and processed for free-floating immunohistochemistry.

In situ hybridization

Retinal sections were processed for single-label immunohistochemistry (IHC) and in situ hybridization

(ISH) experiments or in combination for double-labeling. For IHC, sections were immersed in 0.3% hydrogen peroxide in 0.1M PB for 30 minutes to quench endogenous peroxidases and then placed in blocking buffer (1% bovine serum albumin, 0.1% Triton X-100, 0.1M PB) for 1 hour at room temperature to reduce nonspecific binding. Sections were incubated in fresh blocking buffer containing rabbit polyclonal anti-dsRed (1:500; Clon-Tech Laboratories, Mountain View, CA) at room temperature for 18 hours followed by biotinylated goat antirabbit secondary antibody (1:1,000; Vector Laboratories, Burlingame, CA) in 0.01M phosphate-buffered saline (PBS), 0.1% Triton X-100 (PBST) for 2 hours. Retinal sections were then processed with avidin/biotin reagents (VectaStain Elite Kit, Vector Laboratories) in PBST for 1 hour and developed using 0.04% 3, 3′-diaminobenzidine tetrahydrochloride hydrate (DAB) with 0.006% hydrogen peroxide. Sections were then dehydrated through graded concentrations of alcohol, cleared in xylenes, and coverslipped with Permount mounting medium (Thermo Fisher Scientific). All light microscopy images were captured by a Zeiss Axiophot microscope fitted with a MicroFire camera (Carl Zeiss, Oberkochen, Germany).

For ISH, sections were rinsed in 2× saline-sodium citrate (SSC; 1× SSC is 0.15M sodium chloride and 0.015M sodium citrate, pH 7.0) and acetylated at room temperature in 0.25% acetic anhydride in 0.1M triethanolamine (TEA, pH 8) for 15 minutes. Sections were washed in distilled water, dehydrated in graded concentrations of alcohol, and air-dried for 30 minutes. Each slide was covered with 70 μl hybridization buffer (50% formamide, 10% dextran sulfate, 3× SSC, 1× Denhardt's solution, 0.1 mg/ml yeast tRNA,10 mM dithiothreitol, and 50 mM sodium phosphate buffer, pH 7.4) containing 2.5×10^6 dpm of the 35S-labeled D1R cRNA probe (accession no. NM010076; nucleotides 1484–2196). Sections were coverslipped, loaded into a humidified chamber, and placed in an oven at 55°C for 18 hours. After hybridization, sections were rinsed in 2× SSC and incubated in 200 μg/ml ribonuclease A in 10 mM Tris-HCl, 0.5 M NaCl, pH 8 at 37°C for 1 hour. Stringent washes were performed by incubation in decreasing concentrations of SSC (2×, 1×, and 0.5×) at room temperature followed by 0.1× SSC for 1 hour at 70°C. Sections were washed in distilled water, dehydrated in graded concentrations of alcohol, and air-dried.

To visualize hybridization, sections were loaded into a film cassette with Biomax MR autoradiographic film (Carestream Health, Rochester, NY) and stored for 4–10 days in a darkroom before film development. As a positive control, the D1R cRNA probe was hybridized to thin sections of mouse striatum. The results showed heavy labeling within the caudate/putamen, nucleus accumbens, and olfactory tubercle, and lower levels of signal in the cerebral cortex and septal nucleus (data not shown). We also processed controls to confirm the specificity of D1R mRNA expression in retinal sections. Signal denoting D1R mRNA hybridization was detected in sections incubated with ^{35}S-labeled D1R cRNA antisense probe (Fig. 1B1), but not in retinal sections hybridized to ^{35}S-labeled D1R cRNA sense probe or in sections pretreated with RNAse followed by hybridization to ^{35}S-labeled D1R cRNA antisense probe (Fig. 1B2,B3). These results provide evidence for specific D1R cRNA probe detection of endogenous D1R mRNA.

For combined IHC and ISH, sections were first processed for IHC as described and then fixed again post-DAB development using 4% paraformaldehyde for 15 minutes. Following extensive rinsing, sections were dehydrated in graded concentrations of alcohol and placed in xylenes to remove pap pen residue. Sections were then rehydrated and the ISH procedure was performed as described with successful hybridization verified on autoradiographic film. Sections were dipped in Ilford K5D emulsion (Polysciences, Warrington, PA) for 16–28 days prior to development and coverslipping.

Immunofluorescence and antibody characterization

Retinal thin sections and whole-mount preparations were washed several times in 0.1M PBS and blocked in a solution containing 3% normal donkey serum (NDS) and 0.5% Triton-X 100 in PBS for 1 hour at room temperature. Primary antibodies generated in different host species were diluted in 1% NDS and 0.5% Triton-X 100 in PBS. Sections were incubated with primary antibodies overnight at room temperature and whole-mount preparations with filter paper attached were incubated for 3 days at 4°C. Following primary antibody incubation, retinal tissues were washed and incubated in a mixture of secondary antibodies, conjugated with Alexa 488, 568, 594, or 647 (Life Technologies, Carlsbad, CA) at room temperature for 2 hours. The dilution for secondary antibodies ranged from 1:200–1,000. Sections were washed and coverslipped using ProLong Gold antifade reagent (Life Technologies). The preparation was viewed with a confocal microscope (TCS SP2 or SP8, Leica, Wetzlar, Germany) using a 63× oil, 63× water, or 20× water immersion objective lens. Images were captured at a resolution of 1024×1024 pixels or 1024×256 pixels, with line and frame average setup to 3. The z-step for stack images was 0.3 μm and the zoom factor was 2.5 or 3.0. For double- or triple-

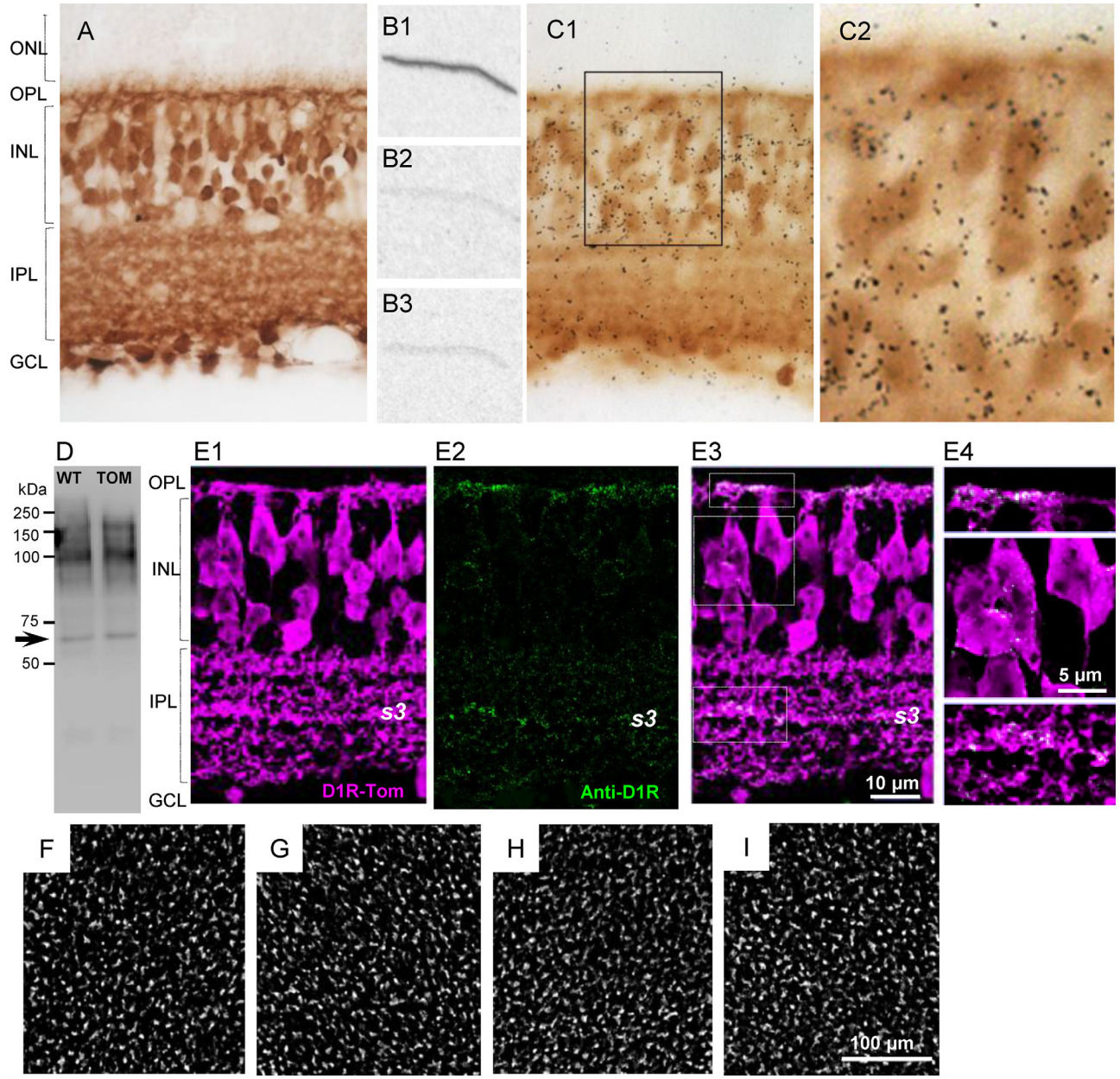

Figure 1. Analysis of retinal preparations from Drd1a-tdTomato transgenic mice. **A**: tdTomato expression in a transverse section. tdTomato was detected using anti-DsRed antibody and DAB staining. **B1**: Autoradiogram from the Drd1a-tdTomato retinal section processed with ^{35}S-labeled D1R cRNA antisense probe that detects D1R mRNA. Radioactivity was not observed in control slices processed with ^{35}S-labeled D1R cRNA sense probe **(B2)** and pretreated with RNAse prior to ^{35}S-labeled D1R cRNA antisense probe incubation **(B3). C1**: tdTomato expression (DAB staining) was overlaid with in situ hybridization using the ^{35}S-labeled D1R cRNA probe (low-power image). **C2**: High-power image from the box in C1. **D**: Western blot of mouse retinas from wildtype (WT) and Drd1a-tdTomato (TOM) immunolabeled with mouse D1R antibody. The arrow shows the reported molecular weight for D1R, between 45–66 kDa. The larger molecular weight bands (~90–150 kDa) may represent dimers in various states of glycosylation (Jarvie et al., 1989; Luedtke et al., 1999). **E1**: tdTomato fluorescence was enhanced with dsRed antibody. **E2**: Punctate D1R immunoreactivity was mainly detected on dendritic process of cone bipolar cells in the OPL and cell processes within the entire IPL, with a stronger immunoreactivity seen in *s3* stratum. Staining was hardly detected in somas in the INL layer. **E3**: D1R immunoreactivity was frequently colocalized with tdTomato positive cell processes. **E4**: High-power image from the box in (E3). **F–I**: tdTomato fluorescence in the INL in whole-mount retinal preparation. The image was captured from different regions of the retina. The distribution of tdTomato-expressing cells was homogeneous across the retina ($n = 2$ mice). [Color figure can be viewed in the online issue, which is available at wileyonlinelibrary.com.]

TABLE 1.
Primary Antibodies

Antibody	Immunogen	Source, Cat. #, Species	RRID	Dilution
Calbindin D-28k	Purified calbindin D-28 from chicken gut	Swant, 300 Mouse monoclonal	AB_10000347	1:1,000
Calsenilin/DREAM, clone 40A5	Full-length GST fusion protein of human Calsenilin	EMD Millipore, 05-756 Mouse monoclonal	AB_2313634	1:2,000
ChAT	Human placental enzyme	EMD Millipore, AB144P Goat polyclonal	AB_2079751	1:200
CtBP2 (E-16)	Peptide near C-terminus of human CtBP2	Santa Cruz Biotechnology, sc-5966 Goat polyclonal	AB_2086774	1:500
Dopamine D1 Receptor	123 amino acid c-terminus of recombinant rat D1a receptor	EMD Millipore, MAB5290 Mouse monoclonal	AB_2094841	1:500
Dab1	Mouse disabled protein (mDab1)	Howell et al., 1997 Rabbit polyclonal	AB_2314280	1:500
dsRed	DsRed-Express	Clontech Laboratories, 632496 Rabbit polyclonal	AB_10013483	1:500
GFP	Green fluorescent protein	EMD Millipore, MAB3580 Mouse monoclonal	AB_94936	1:500
HCN1 clone N70/28	Fusion protein amino acids 778-910 at C-terminus of rat HCN1	NeuroMab, 75-110, Mouse monoclonal	AB_2115181	1:200
HCN4 clone N114/10	Fusion protein amino acids 1019-1108 at C-terminus of rat HCN4	NeuroMab, 75-150 Mouse monoclonal	AB_2248534	1:200
NK3R	Amino acids 410-417 of rat neurokinin3 receptor (NK3R)	Gift from Dr. Hirano Rabbit polyclonal	AB_2314947	1:700
OPN1SW (N-20)	N-terminus of human OPN1SW	Santa Cruz Biotechnology, sc-14363 Goat polyclonal	AB_2158332	1:1,000
PKA RIIβ	Amino acids 1-418 of human PKA RIIβ	BD Biosciences, 610625 Mouse monoclonal	AB_397957	1:3,000
PKC α	Amino acids 645-672 at C-terminus of human PKC α	Santa Cruz Biotechnology, sc-8393 Mouse monoclonal	AB_628142	1:500
Ribeye, B domain	Synthetic peptide, amino acids 974-988 of rat ribeye	Synaptic Systems, 192003 Rabbit polyclonal	AB_2261205	1: 10,000
Synaptotagmin-2	Zebrafish Syt2	ZIRC, znp-1 Mouse monoclonal	AB_10013783	1:200
TH	Purified TH from PC12 cells	Gift from Dr. Kapatos Mouse monoclonal (LNC1)	AB_2201528	1:500

labeled tissue, the sequential scanning was performed to eliminate crosstalk between channels and to separate signals from each other.

Details of the primary antibodies used are provided in Tables 1 and 2. In transgenic mouse lines, anti-GFP and anti-dsRed were used to obtain stronger GFP/YFP signals and tdTomato fluorescence, respectively. All antibodies were purchased from vendors or gifted from scientists. All antibodies have been characterized and are listed in JCN (RRID). Dopamine D1 receptor, CtBP, and ribeye antibodies were characterized and compared to previous reports (Figs. 1D, 5B).

Protein isolation and western blot

Retinas from Drd1a-tdTomato ($n = 2$) and C57BL/J6 ($n = 2$) wildtype mice were dissected and placed in ice-cooled radioimmunoprecipitation assay (RIPA) buffer (Thermo Scientific, cat. no. 89900) and homogenized. Protein concentrations were determined using the BCA Protein Assay Kit (Thermo Fisher Scientific, cat. no. 23227) and 80 μg protein samples were run on 10% acrylamide gels. After electrophoretic separation, proteins were transferred onto polyvinylidene (PVDF) membranes (Bio-Rad Laboratories, Hercules, CA) for 90 minutes at a constant voltage of 150 V. Membrane was blocked in 8% dry milk in 1× TBS/Tween 20 (TBST) for 1 hour at room temperature then incubated overnight at 4°C in primary antibody, monoclonal mouse anti-D1R, diluted 1:500 in 1× TBST with 4% milk. After several washes, the membrane was incubated in secondary goat antimouse antibody conjugated to horseradish peroxidase (HRP) (cat. no. 554002, BD Biosciences, San Jose, CA) diluted 1:1,000 in 1× TBST with 4% milk for 1 hour at room temperature. Protein bands were detected using chemiluminescent HRP substrate (WBKLS0100, Millipore) and imaged on a Fluorochem E imager (Protein Simple, San Jose, CA).

TABLE 2.
Synthetic Peptide Immunogenic Information

Antibody	Source, cat. #	Immunogen peptide
CtBP2 (E-16)	Santa Cruz Biotech., sc-5966	Human CtBP, 369-419 Amino acids TPHTAWYSEQASLEMREAAATEIRRAITGRIPESLRNCVNKEFEVTSAPWS
OPN1SW(N-20)	Santa Cruz Biotech., sc-14363	Human OPN1SW, 8-58 Amino acids FYLFKNISSVGPWDGPQYHIAPVWAFYLQAAFMGTVFLIGFPLNAMVLVA
PKC α	Santa Cruz Biotech., sc-8393	Human PKC α, 622-672 Amino acids MTKHPAKRLGCGPEGERDVREHAFFRRIDWEKLENREIQPPFKPKVCGKG

Neurobiotin injection

Retinal slice preparations were made using oxygenated HEPES buffered solution. The retina was isolated from the eye-cup, placed on a piece of filter membrane (HABG01300, Millipore), and cut into slices (250 μm thickness) using a hand-made chopper. The retinal preparations were stored in an oxygenated box at room temperature. For neurobiotin injection, each slice preparation was transferred to a chamber on a microscope stage and perfused with Ames' medium buffered with $NaHCO_3$ (294 mOsm) (Sigma, St. Louis, MO), which was continuously bubbled with 95% O_2 and 5% CO_2 (pH 7.4 at 30°C). The intracellular solution contained the following (in mM): 111 K-gluconate, 1.0 $CaCl_2$, 10 HEPES, 1.1 EGTA, 10 NaCl, 1.0 $MgCl_2$, 5 ATP-Mg, and 1.0 GTP-Na, adjusted to pH 7.2 with KOH (269 mOsm). A fluorescent dye, sulforhodamine B (0.005%, Sigma), and neurobiotin (0.5%, Vector Laboratories) were included in the pipette solution. Whole-cell patch recordings were made from tdTomato stained cell somata in retinal slices by viewing them with an upright microscope (Slicescope Pro 2000, Scientifica, East Sussex, UK) equipped with a charge coupled device (CCD) camera (Retiga-2000R, Q-Imaging, Surrey, BC, Canada). Whole-cell recordings were continued for 10–15 minutes to ensure that the neurobiotin filled the entire cell. Electrodes were pulled from borosilicate glass (1B150F-4; World Precision Instruments, Sarasota, FL) with a P1000 Micropipette Puller (Sutter Instruments, Novato, CA) and had resistances of 7–11 MΩ. Immediately after whole-cell recording, a sulforhodamine B image was captured using the CCD camera to photograph the live retinal preparation. After dye injection, the slice preparation was fixed using 4% paraformaldehyde for 30 minutes, incubated with streptavidin-conjugated Alexa 488 (1:200, Life Technologies), rabbit anti-DsRed (1:500, ClonTech Laboratories), and goat anti-ChAT antibody (1:200, EMD Millipore) overnight at room temperature. Then the preparation was incubated with donkey secondary antibodies: Alexa 568 antirabbit and Alexa 647 antigoat (Life Technologies) for 2 hours at room temperature. The slice preparation was carefully placed on a histo-bond slide, which was sealed with anti-fade reagent (ProLong Gold, Life Technologies) and coverslipped.

Data analysis

D1R mRNA expression in the ISH experiments was analyzed by counting silver grains within a 6.6-μm circle positioned over the center of tdTomato-positive ($n = 171$) or tdTomato-negative ($n = 103$) somata across the inner nuclear layer (INL) from the vertical retinal sections processed for combined IHC and ISH. The numbers of grains per tdTomato-positive or -negative cell were averaged across nine retinal images obtained from three tdTomato mice and compared by paired *t*-test (alpha <0.05).

Image analysis was performed using AutoQuant X3 and Image-Pro Premier 3D software (Media Cybernetics, Rockville, MD). We used the deconvolution, 3D, and colocalization analysis functions. For image deconvolution, spherical aberration was autodetected for each channel based on objective lens immersion refractive index (RI), specimen mounting medium RI and distance from the coverslip. The 3D confocal images were then deconvoluted.

Cell markers and tdTomato fluorescence colocalization was initially examined by rotating the 3D images and by analyzing series of single optical sections (0.3-μm thick) from collected *z*-stack images. We also used mathematical analysis. For OFF bipolar cells, we measured fluorescent intensities of both markers and tdTomato across somas using AutoQuant X3. Brightness of images was set at subsaturated levels. Arbitrary fluorescence of both markers and tdTomato was normalized to the maximum intensity of cell markers, and plotted across the cell (edges designated 0% and 100%).

For small objects such as CtBP puncta colocalization analysis, we performed 2D cross-correlation coefficient analysis using a custom MatLab (MathWorks, Natick, MA) code (T.I. wrote) (Soto et al., 2011; Zinchuk et al., 2011). Images of CtBP puncta and HCN1 were excised (3 × 3 μm). Single digital sections (0.3 μm) of two colors were separated into two grayscale images. Background noise levels were reduced to 0 levels. 2D correlation coefficient program compares two images dot by dot using the equation:

$$R(i,j) = \frac{c(i,j)}{\sqrt{c(i,i)c(j,j)}} \quad (1)$$

The maximum of correlation coefficient is 1. The correlation coefficient of images was compared to that of

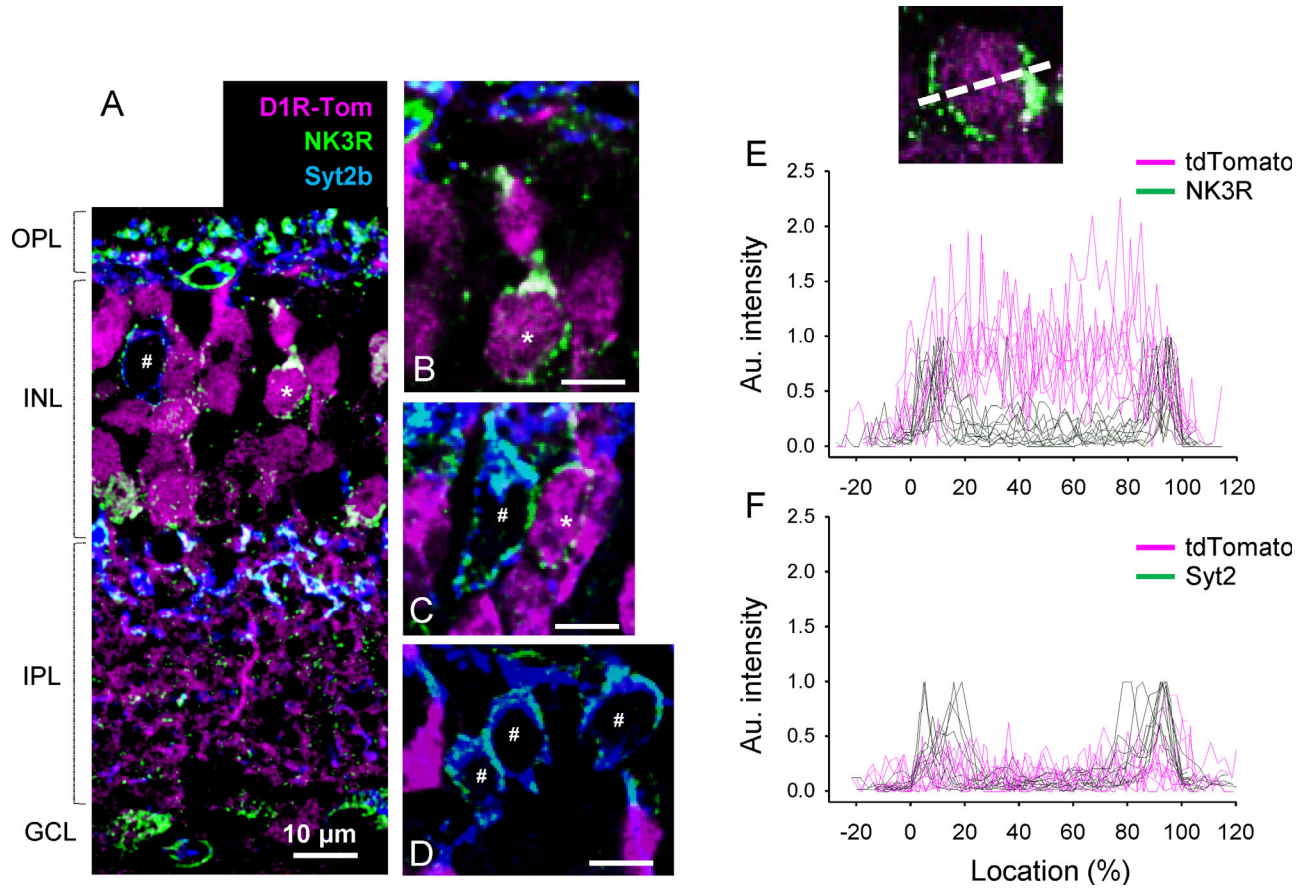

Figure 2. tdTomato expression in type 1 and 2 OFF bipolar cells. **A**: NK3R antibody labeled type 1 and 2 OFF bipolar cells. Type 1 cells, identified with NK3R but not Syt2b antibodies, were colocalized with tdTomato (*). Type 2 cells were labeled with both NK3R and Syt2b, but were negative for tdTomato (#). **B**: A magnified view of a type 1 cell soma. All magnified views in this and subsequent figures are excised from single digital section images (0.3–0.5 µm thickness). **C**: Somas of type 1 and type 2 cells. Only the type 1 cell colocalized with tdTomato. **D**: Three somas of type 2 cells showed no colocalization with tdTomato fluorescence. **E**: Fluorescent intensities of tdTomato and bipolar cell markers were measured across somas (inset) ($n = 8$) as described in the Materials and Methods. For type 1 bipolar cells, NK3R labeled the cellular edges while tdTomato fluorescence was observed across the entire soma. Some type 1 cells were not labeled with tdTomato. **F**: Fluorescent intensity measurement showed that type 2 cell somas did not colocalize with tdTomato ($n = 10$). Scale bars = 5 µm in B–D. [Color figure can be viewed in the online issue, which is available at wileyonlinelibrary.com.]

images when one channel was rotated 90°. The correlation coefficient was plotted in 3D mesh graph using MatLab.

RESULTS

Drd1a-tdTomato mouse

Dopamine is a key molecule for retinal daytime function. We used the Drd1a-tdTomato line 6 BAC transgenic reporter mouse to investigate cell-type specificity of D1R expression in the retina. These mice express tdTomato fluorescence driven by the D1R gene locus, as demonstrated in medium spiny neurons of the striatum known to express the endogenous D1R (Ade et al., 2011; Thibault et al., 2013).

Within the retina, expression of tdTomato was observed in cell bodies of many neurons located in the INL and ganglion cell layer (GCL), as well as dendrites and axons in both the outer plexiform layer (OPL) and the IPL (Fig. 1A). No tdTomato was found in photoreceptors in the outer nuclear layer (ONL). To determine whether tdTomato was localized to authentic D1R neurons, we performed ISH using ^{35}S-labeled D1R cRNA probes on retinal sections double-labeled for tdTomato immunoreactivity. The probe was tested on the retinal sections (Fig. 1B1–B3). Silver grains within the emulsion layer indicative of endogenous D1R mRNA expression were concentrated over the majority of tdTomato positive soma (Fig. 1C1,C2). In neurons of the INL, 10.18 ± 0.3 grains were associated with tdTomato-positive soma compared to 3.49 ± 0.2 grains found

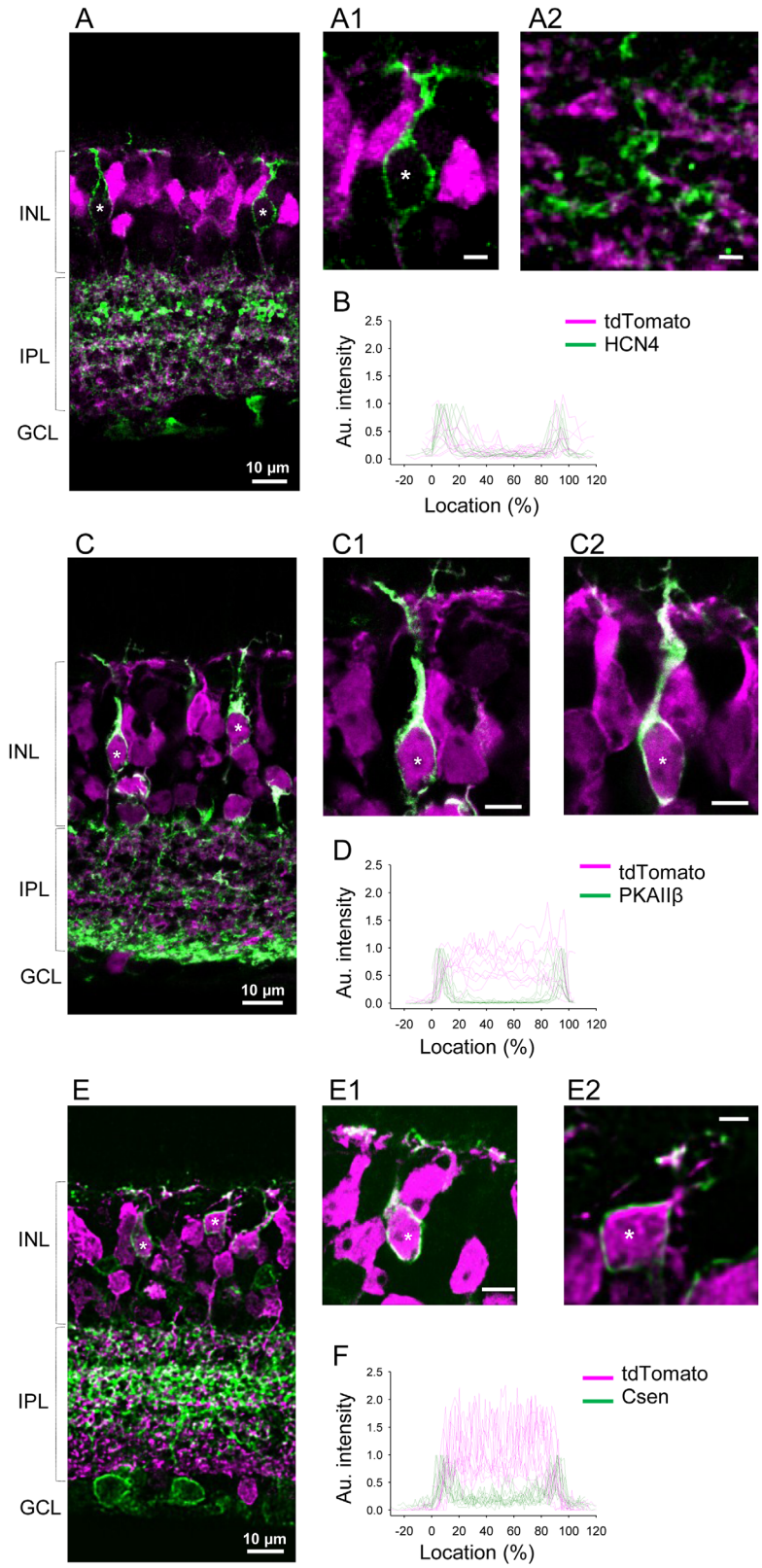
A
A1
A2
INL
IPL
GCL
10 µm
B
tdTomato
HCN4
Au. intensity
Location (%)
C
C1
C2
D
tdTomato
PKAIIβ
E
E1
E2
F
tdTomato
Csen

Figure 3.

over tdTomato-negative cells ($P < 0.0001$, paired *t*-test, $n = 3$ mice). Grains observed in the area of tdTomato-negative cells might be attributable to mRNA transport through axons/dendrites (Kindler et al., 2005), or background noise. Nevertheless, the grains were highly concentrated over tdTomato-positive cells, indicating that D1Rs are primarily expressed in tdTomato cells of the retina.

We also analyzed whether tdTomato-expressing cells colocalized with D1R immunoreactivity. The specificity of this antibody in mouse retinal tissue was assessed by immunoblot (Fig. 1D) and found to be consistent with previous reports (Jarvie et al., 1989; Luedtke et al., 1999). D1R immunoreactivity was observed in the OPL and part of the IPL ($n = 3$ mice, Fig. 1E1–E4). Punctate D1R immunostaining was mainly colocalized with processes of tdTomato-expressing cells both in the OPL and IPL, with stronger immunoreactivity seen in the *s3* stratum; examples of nonlocalization were much less frequent. However, signal was difficult to observe in the soma region of the INL (Fig. 1E2–E4), making it impossible to identify the morphologies of cells expressing D1Rs unless combined with tdTomato-immunofluorescence. We also examined tdTomato-expressing cells using whole-mount retinal preparation (Fig. 1F-I) and found similar distributions of cellular tdTomato fluorescence across central versus peripheral retina. Taken together, both the ISH and IHC results indicate that tdTomato-positive cells express endogenous D1R, and that the tdTomato transgenic mouse offers advantages for investigating D1R-expressing cells of the retina.

OFF cone bipolar cells

Thirteen types of bipolar cells have been identified, including five types of OFF bipolar cells, seven types of ON bipolar cells, and a single rod bipolar cell type (Helmstaedter et al., 2013; Ichinose et al., 2014). OFF bipolar cell types can be identified with specific antibodies (Wässle et al., 2009). We used immunolabeling techniques to examine OFF bipolar cell types that colocalize with tdTomato. All OFF bipolar cell markers labeled particular bipolar cells as well as subsets of amacrine cells and ganglion cells. These cells ramify their processes and dendrites in the IPL, which obscured bipolar cell axon terminal colocalization with tdTomato fluorescence. Thus, we analyzed bipolar cell dendrites and somas in order to determine colocalization with tdTomato.

First, an anti-neurokinin 3 receptor (NK3R) antibody was used to identify both type 1 and 2 OFF bipolar cells. Synaptotagmin 2b (Syt2b) colabeling was employed to distinguish type 2 OFF bipolar cells (Fig. 2A–D). All type 1 OFF bipolar cells (*, NK3R-only) were found to colocalize with tdTomato, an observation that was confirmed with fluorescence intensity analysis (18 cells, $n = 2$ mice; Fig. 2E). Type 2 OFF bipolar cells, labeled both with NK3R and Syt2b antibodies, were all tdTomato negative (78 cells, $n = 4$ mice; Fig. 2F).

Second, other antibodies were used that were selective for single types of OFF bipolar cells, and we were able to determine tdTomato colocalization. Type 3a bipolar cells were labeled with HCN4, which were all tdTomato-negative (22 cells, $n = 3$ mice; Fig. 3A–B). Type 3b cells were labeled with protein kinase A (PKA) RIIβ, which were all tdTomato-positive (56 cells, $n = 3$ mice; Fig. 3C,D). Type 4 cells were labeled with calsenilin (Csen), which were all tdTomato-positive (81 cells, $n = 3$ mice; Fig. 3E,F).

To verify the colocalization of OFF bipolar cell markers with tdTomato, we compared fluorescence levels between outside of cells (–20 to 0% location in Figs. 2E,F, 3B,D,F) and the center of the cells (40 to 60% location in Figs. 2E,F, 3B,D,F). Type 1, 3b, and 4 cells exhibited significantly higher intensity in the inside as compared to outside of the cell ($P < 0.01$ for all three types, paired *t*-test), indicating that these cells colocalize tdTomato protein. In contrast, tdTomato intensities of type 2 and 3a cells were similar between baseline (outside) and the inside of cells ($P = 0.2$ for type 2, $P = 0.09$ for type 3a, paired *t*-test) indicative of no colocalization. Collectively, these data suggest D1R was expressed in OFF bipolar cells in a type-dependent manner: types 1, 3b, and 4 were D1R-expressing bipolar cells, whereas types 2 and 3a were D1R-negative.

ON bipolar cells

The investigation of tdTomato colocalization with ON bipolar cell types was challenging because

Figure 3. tdTomato expression in type 3 and 4 OFF bipolar cells. **A**: HCN4 labeled type 3a OFF bipolar cells did not colocalize with tdTomato (*). **A1**: A magnified view shows a soma of a 3a OFF bipolar cell. **A2**: A magnified view shows axon terminals of a 3a OFF bipolar cell. **B**: Fluorescent intensity measurements confirmed no tdTomato fluorescence in HCN4-labled cells ($n = 10$). **C**: PKA RIIβ-labeled type 3b OFF bipolar cells were positive for tdTomato (*). **C1,C2**: Magnified views show somas of type 3b OFF bipolar cells that are colocalized with tdTomato fluorescence. **D**: Fluorescent intensity measurement revealed tdTomato fluorescence in type 3b OFF bipolar cell somas ($n = 10$). **E**: Calsenilin (Csen)-labeled type 4 OFF bipolar cells were colocalized with tdTomato (*). **E1,E2**: Magnified views show that type 4 OFF bipolar cell somas colocalized with tdTomato. **F**: Fluorescent intensity measurement confirmed tdTomato fluorescence in type 4 OFF bipolar cell somas ($n = 11$). Scale bars = 3 μm in A1, A2, E2, and 5 μm in C1, C2, E1. [Color figure can be viewed in the online issue, which is available at wileyonlinelibrary.com.]

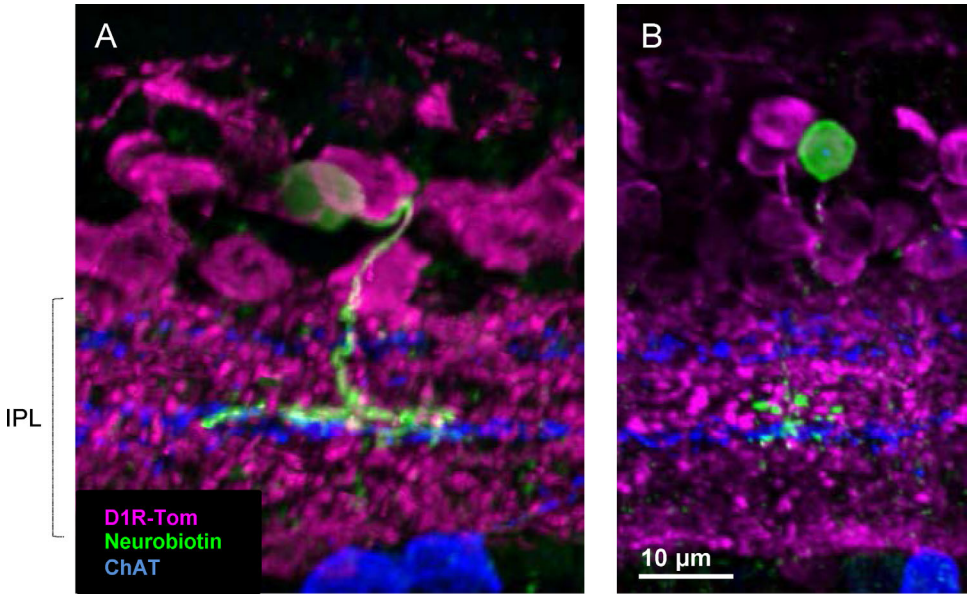

Figure 4. Neurobiotin labeled different sets of type 5 ON bipolar cells. **A**: A type 5-XBC ON bipolar cell with wide axon terminals colocalized with tdTomato. **B**: A type 5 ON bipolar cell with compact axon terminals did not colocalize with tdTomato. ChAT band staining is shown for the IPL sublayers. [Color figure can be viewed in the online issue, which is available at wileyonlinelibrary.com.]

immunomarkers are only available for type 6 cells (Wässle et al., 2009). We overcame this limitation with a combination of transgenic reporter mice, neurobiotin injections, and IHC to characterize D1R expression in ON bipolar cells.

Type 5 cells are defined as ON bipolar cells whose axon terminals ramify between the ON-OFF border (~40% of the IPL depth) and the ON choline acetyltransferase (ChAT) band (stratum 3 or S3) (Ghosh et al., 2004). Different sets of type 5 cells have been recognized in many species of the retina (Ghosh et al., 2004; Fyk-Kolodziej and Pourcho, 2007; Helmstaedter et al., 2013; Ichinose et al., 2014). We distinguished three sets of type 5 cells in the mouse retina using morphological and physiological analyses (Ichinose et al., 2014). Type 5-1 cells responded to light with sustained kinetics and had narrowly ramified axon terminals. Type 5-2 cells were transiently responding cells with wider axon terminals. Finally, type 5-XBC cells exhibited the widest pattern of axon ramification in a monolayer fashion, as reported originally by Helmstaedter et al. (2013). These cells also responded to light transiently similar to type 5-2 cells. In addition, we found that type 5-2 and XBC cells express Na^+ channels and HCN channels (submitted).

To investigate whether type 5 cells colocalized with tdTomato, we initially tried neurobiotin injection. We labeled five type 5 cells; three cells colocalized with tdTomato (Fig. 4A). Two other cells did not colocalize with tdTomato (Fig. 4B). The former resembled type 5-XBC and the latter looked like the type 5-1 cell. However, because of the inefficiency of neurobiotin injection to label type 5 cells, we sought an additional approach to identify this cell type.

Immunostaining with the hyperpolarization-activated cyclic nucleotide-gated potassium channel 1 (HCN1) antibody revealed HCN1 localization near the ON ChAT band where axon terminals of type 5 ramify (Fig. 5A) (Muller et al., 2003; Cangiano et al., 2007). We tested whether HCN1 signaling was a marker for a subset of type 5 cells and if these cells colocalized with tdTomato. HCN-1 immunoreactivity was observed in the entire IPL, with strong signals in the *s3* stratum (Fig. 5A). To examine whether HCN1 immunoreactivity colocalized with bipolar cell terminals, we used CtBP2 antibody, a ribbon synapse marker. CtBP2 antibody was verified (Materials and Methods, Fig. 5B1,B2). We found that the majority of CtBP puncta in the area colocalized with strong HCN1 signaling (Fig. 5C,D), which was confirmed by 2D correlation coefficient analysis (Fig. 5F). This result suggested that HCN1 is a type 5 ON bipolar cell marker. We conducted neurobiotin injection to individual type 5 cells and found that type 5-2 and XBCs colocalized with bright HCN1 signaling (submitted). HCN1 strong signaling completely colocalized with tdTomato fluorescence, indicating that type 5-2 and XBCs express D1Rs (Fig. 5E,G).

We investigated whether type 5-1 cells also colocalized with tdTomato. We counted CtBP2 puncta in a layer of the IPL where HCN1 strong immunoreactivity

was observed. We found that the majority of CtBP puncta in the layer colocalized with HCN1 signaling and a portion of the puncta did not colocalize with HCN1 (Fig. 5D,H). The minor portion of CtBP puncta without HCN1 immunoreactivity (15.3 ± 1.2%, $n = 12$ fields) is likely from type 5-1 bipolar cells because type 5-2 and XBC cells colocalized with HCN1. We also counted CtBP puncta with tdTomato fluorescence at the same layer near ON ChAT band. Similarly, a portion of CtBP (18.7 ± 1.4%, $n = 10$ fields) did not colocalize with tdTomato (Fig. 5I). No differences were observed between CtBP puncta versus HCN1 and the puncta versus tdTomato ($P = 0.08$), suggesting that type 5-1 cells did not colocalize with tdTomato. Taken together, these results suggest that type 5-1 cells did not express D1Rs.

Colocalization of type 6 bipolar cells with tdTomato was examined using Syt2b, a marker for types 2 and 6 of bipolar cells (Fig. 6A1). Entire structures of type 2 cells were intensely labeled, while only axon terminals of type 6 cells were observed in the inner portion of the IPL (Fig. 6A) (Wässle et al., 2009). Syt2b-positive type 6 axon terminals colocalized with tdTomato ($n = 3$ mice, 20 fields; Fig. 6A2,A3). This was confirmed with 2D cross-correlation coefficient analysis (Fig. 6B). This observation was consistent with neurobiotin staining of type 6 cells ($n = 4$ cells, data not shown), indicating that type 6 ON bipolar cells express D1Rs.

To investigate type 7 bipolar cells and tdTomato colocalization, we used the Gus-GFP mouse line (Huang et al., 1999, 2003) in which type 7 bipolar cells are strongly GFP-positive and rod bipolar cells (RBCs) are weakly labeled (Fig. 6C). We generated double transgenic mice with Drd1a-tdTomato line 6 and Gus-GFP strains and examined evidence for GFP and tdTomato colocalization (Fig. 6C1-C3). The majority of type 7 GFP cells were tdTomato-positive (91/95 cells, 96%, 3 mice), indicating that type 7 ON bipolar cells express D1Rs. In contrast, all GFP-positive RBCs were negative for tdTomato (117cells, $n = 3$ mice).

Types 8 and 9 cells are fewer in number compared to other types (Haverkamp et al., 2005; Helmstaedter et al., 2013), and our tdTomato-targeted neurobiotin injections did not label them. Type 9 bipolar cells receive synaptic inputs exclusively from genuine S-opsin-expressing cone photoreceptors (S-cones) (Haverkamp et al., 2005). We therefore investigated if tdTomato-expressing cells extended their processes to the genuine S-cone terminals. In the mouse retina, M- and S-opsin-expressing cones are unevenly distributed (Szel et al., 1992; Haverkamp et al., 2005). Both M- and S-opsin-expressing mixed cones are located on the ventral side of the retina. In the dorsal retina, the majority of cones are genuine M-opsin-expressing cells, while the minority are genuine S-cones (Haverkamp et al., 2005). We used an S-opsin antibody to label genuine S-cones in the dorsal retina and investigated processes of tdTomato-expressing cells. A small number of the S-cone terminals were labeled in dorsal retinal sections (Fig. 7A), whereas many cones were labeled with S-opsin in the ventral retina (Fig. 7B), indicating genuine S-cones on the dorsal side and mixed-S and M cones on the ventral side. We detected tdTomato-stained processes attached to the genuine S-cones (Fig. 7A, inset).

To investigate whether the tdTomato-labeled processes were from type 9 bipolar cells, we generated double transgenic mice from tdTomato-Drd1a and the Clomeleon 1 (Clm 1-YFP/CFP) transgenic mouse line, in which YFP fluorescence was observed in type 9 cells (Haverkamp et al., 2005). We confirmed that type 9 bipolar cells extended dendrites toward the genuine S-cones, and did not colocalize with tdTomato expression ($n = 15$ cells, 4 mice, Fig. 7C1–C3). These results indicate that type 9 bipolar cells are tdTomato negative and do not express D1Rs. Processes of tdTomato-expressing cells attaching to genuine S cone terminals were from other types of bipolar cells, such as types 2, 3, 4, and 7 or horizontal cells (Fig. 7D,E) (Breuninger et al., 2011).

Finally, we used a protein kinase C alpha (PKCα) antibody to examine D1R expression in rod bipolar cells (RBCs). RBCs did not colocalize with tdTomato-expressing cells (104 cells, $n = 3$ mouse; Fig. 8A), which is consistent with the results in Figure 6C and a previous report (Veruki and Wässle, 1996). Taken together, D1Rs were expressed in bipolar cell types 1, 3b, 4, 6, and 7, but not in types 2, 3a, 9, or rod bipolar cells. Three groups of type 5 cells expressed D1Rs differently: XBCs and type 5-2 cells expressed D1Rs, whereas type 5-1 cells did not colocalize with D1R-tdTomato fluorescence.

Horizontal cells and AII amacrine cells

We also examined whether horizontal cells and AII amacrine cells colocalized with tdTomato because gap junctions in horizontal cells are controlled by dopamine and AII-AII couplings might be controlled by ON bipolar cell activity (Hampson et al., 1992; Bloomfield and Volgyi, 2009; Kothmann et al., 2012). We used a calbindin antibody to label horizontal cells. Although tdTomato expression was relatively weaker in horizontal cells as compared to tdTomato expression in bipolar cells, calbindin-immunoreactive horizontal cells colocalized with tdTomato ($n = 16$ cells, 100%, $n = 2$ mice; Fig. 8B1–B3).

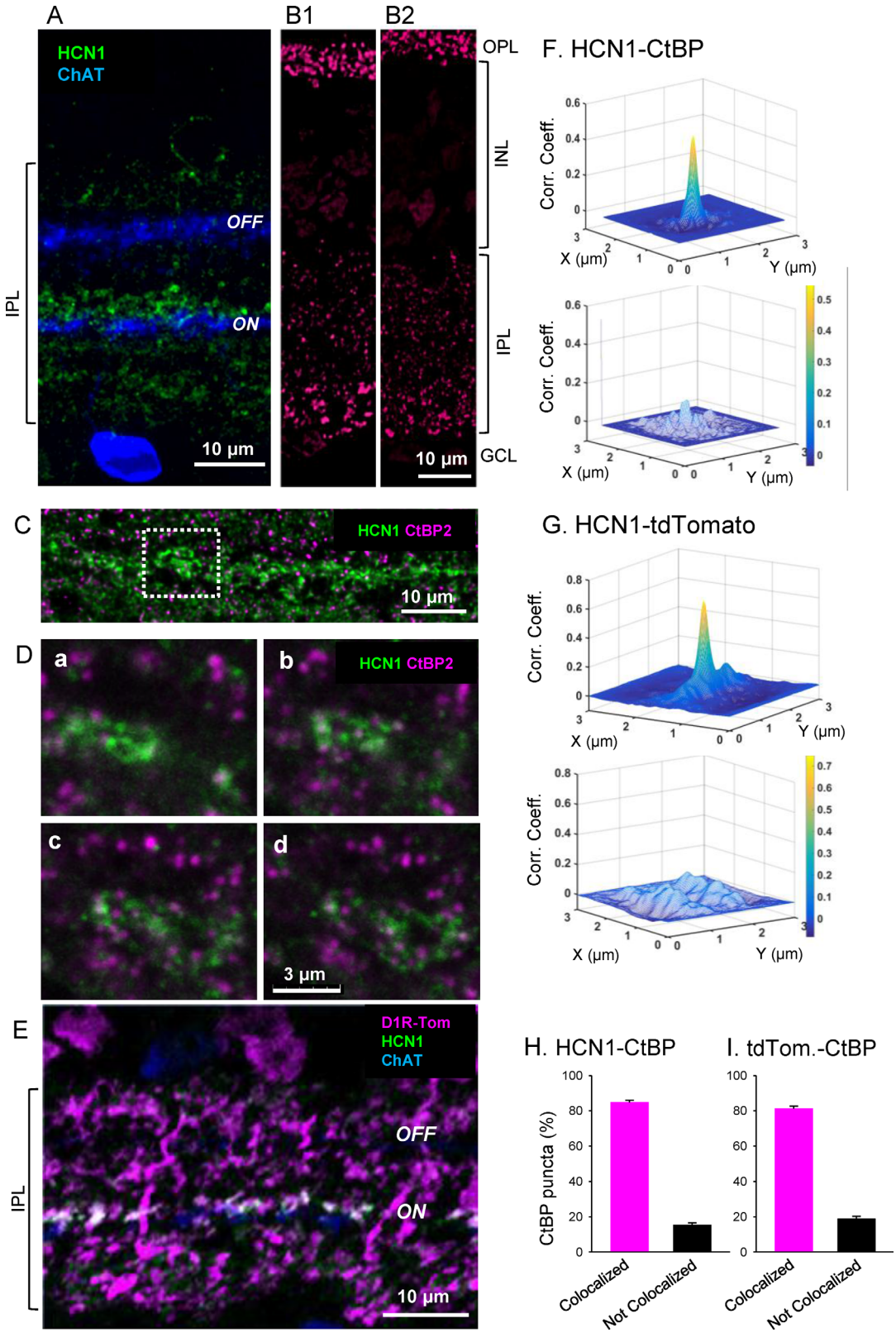
A
B1
B2
HCN1
ChAT
OFF
ON
IPL
10 µm
OPL
INL
IPL
GCL
F. HCN1-CtBP
Corr. Coeff.
X (µm)
Y (µm)
C
HCN1 CtBP2
10 µm
G. HCN1-tdTomato
D
a
b
c
d
3 µm
E
D1R-Tom
HCN1
ChAT
H. HCN1-CtBP
I. tdTom.-CtBP
CtBP puncta (%)
Colocalized
Not Colocalized

Figure 5.

We used disabled-1 (dab-1) antibody to specifically label AII amacrine cells in mouse retina (Rice and Curran, 2000) and investigated whether dab-1-immunolabeled AII cells colocalized with tdTomato. Our results showed that the majority of dab-1-immunoreactive cells were not colocalized with tdTomato (arrows in Fig. 8C1–C3), suggesting that AII amacrine cells do not express D1Rs. However, ~25% of dab-1-labeled cells were positive for tdTomato (10 out of 41 cells, $n = 2$ mice; arrowheads in Fig. 8C1–C3). We decided to perform another experiment to confirm this result. It is known that AII amacrine cells are surrounded by dopaminergic fibers that are immunoreactive for tyrosine hydroxylase (TH) and form ring-like structures around AII somas at the INL/IPL border (Voigt and Wässle, 1987; Volgyi et al., 2014). In whole-mount retinal preparations, we observed TH ring-like formations and the majority of rings were not filled with tdTomato cells (asterisks in Fig. 8D1,D2). However, ~25% of the ring formations ($n = 7$ fields) were occupied by tdTomato-positive somas (triangles in Fig. 8D1,D3). Taken together, the majority of AII amacrine cells were D1R-negative, while about 25% of AII cells were immunoreactive for tdTomato, indicating that they express D1Rs.

DISCUSSION

Drd1a-tdTomato line-6 BAC transgenic mouse

Bacterial artificial chromosome (BAC) technology is a method by which large regions of DNA can be introduced into the mouse genome via recombination-mediated genetic engineering. However, BACs may contain "extra" genes in addition to the original target gene. The Drd1a-tdTomato line 6 contains an extra gene, Sfxn1. Further experiments revealed that this unwanted extra gene does not alter the fidelity of tdTomato expression in the correct cell population (Ting and Feng, 2014). tdTomato fluorescence is limited to D1R-expressing cells as previously confirmed in the striatum (Ade et al., 2011) and so we took advantage of this mouse to examine cell-type specific D1R expression in the retina.

Because the Drd1a-tdTomato mouse line has not been used for retinal research, we used ISH and a D1R antibody to verify that D1R signals colocalized with tdTomato (Fig. 1). We found evidence for mRNA colocalization in tdTomato-positive cells, as well as processes labeled with the D1R antibody that also colocalized with tdTomato fluorescence (Fig. 1). These data confirm D1R expression in tdTomato-expressing cells of the retina. tdTomato fluorescence was observed in the dendrites, somas and axon terminals in most neurons (Figs. 2–6, and 8) while the D1R antibody stained mainly processes in the IPL (Fig. 1E2). These findings demonstrate that this mouse line is a useful tool for analyzing D1R-expressing cells in the retina.

D1 receptor expression in retinal bipolar cells

D1R expression in bipolar cells has not been well studied. Veruki and Wässle (1996) analyzed D1 receptor immunoreactivity in the rat retina and found that type 5, 6, and 8 cone bipolar cells and horizontal cells were D1R-immunoreactive, whereas type 2 and rod bipolar cells, and ChAT, TH, and AII amacrine cells were not immunoreactive. Assuming that bipolar cell types are equivalent in rat and mouse retinas, our results are consistent with this previous report: type 6 and a subset of type 5 are positive, whereas type 2, RBCs, TH cells are negative.

Mora-Ferrer et al. (1999) and Nguyen-Legros et al. (1997) used a D1R antibody in goldfish, rat, and mouse retinas and observed D1R immunoreactivity in INL cells and the IPL; however, the cell types were not clearly determined. Witkovsky et al. (2007) investigated the

Figure 5. Evidence that HCN1 antibody labels type 5 cells and colocalized with tdTomato. **A**: HCN1 signaling was observed in the IPL near the outer edge of the ON ChAT band. **B**: Verification of CtBP antibody. CtBP2/Ribeye antibodies labeled ribbon synapses in mouse retinal sections. Puncta of ribbon synapses in photoreceptors are labeled in the OPL, while ribbon synapses in bipolar cell terminals are labeled throughout the IPL. Both anti-CtBP2 from Santa Cruz **(B1)** and anti-Ribeye from Synaptic Systems (**B2;** Table 1) showed similar pattern that are also consistent with the immunostaining reported in mouse retina with different Ribeye antibody (fig. 1, tom Dieck et al., 2005). **C**: HCN1 signaling overlaps with a ribbon synapse marker, CtBP, showing labeled puncta. **D**: High-power view showing HCN1 staining and CtBP puncta from the dashed box illustrated in C. All panels are single digital section images (0.3 μm thick). From **a–d**, images were taken from one side to another side of the HCN1 strong staining every 1 μm. Many CtBP puncta colocalized with HCN1, indicating that HCN1 colocalized with bipolar cell terminals. **E**: Strong HCN1 staining also colocalized with tdTomato staining immediately next to the ON ChAT band. **F**: 2D cross-correlation coefficient analysis of CtBP puncta and HCN1 signaling. The majority of CtBP2 puncta colocalized with HCN1 staining ($n = 25$ puncta with HCN1 colocalization; upper). A 90° rotation of the HCN1 image reduced the correlation coefficient (lower panel) indicating that HCN1/CtBP2 colocalization was not random. **G**: 2D cross-correlation coefficient analysis of tdTomato and HCN1 signaling. Correlation was detected ($n = 20$ images; upper panel), whereas no correlation was observed when one channel was rotated 90° (lower panel). **H**: CtBP puncta were expressed as the proportion of puncta colocalized with HCN1 or not colocalized with HCN1 (1,217 puncta were analyzed from 12 images, $n = 3$ animals). **I**: CtBP puncta were expressed as the proportion of puncta colocalized with tdTomato or not colocalized with tdTomato (955 puncta were analyzed from 9 images, $n = 3$ animals). [Color figure can be viewed in the online issue, which is available at wileyonlinelibrary.com.]

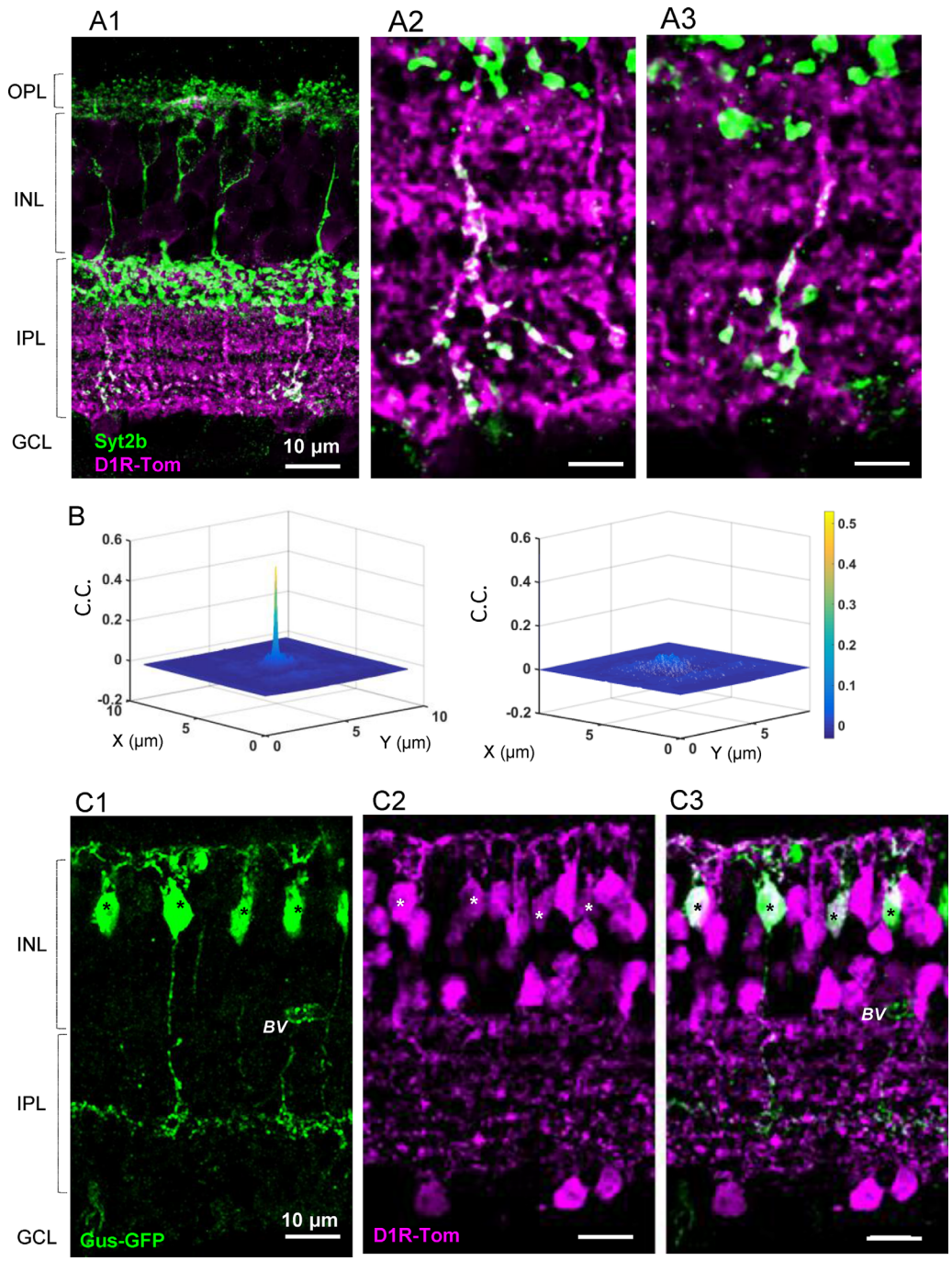

Figure 6. Both type 6 and 7 ON bipolar cells colocalized with tdTomato fluorescence. **A1**: Syt2b labeled axon terminals of type 6 cells and the entire structure of type 2 OFF bipolar cells (dendrites-somas-axons). Only axon terminals of type 6 cells colocalized with tdTomato. **A2,A3**: Magnified views of type 6 axon terminals with tdTomato fluorescence in a single digital section (0.3 µm thick). **B**: (left) 2D cross-correlation coefficient showed that tdTomato fluorescence colocalized with syt2b-stained type 6 axon terminals ($n = 20$ fields). (right) A 90° rotation of the green channel resulted in no correlation. **C1–C3**: Double transgenic mice with Gus-GFP (C1) and Drd1a-tdTomato (C2) revealed that type 7 ON bipolar cells colocalized with tdTomato (C3). *Double-labeled cells; BV, blood vessel. Scale bars = 3 µm in A2, A3, and 10 µm in C2, C3. [Color figure can be viewed in the online issue, which is available at wileyonlinelibrary.com.]

immunoreactivity of DARPP-32, a downstream signaling regulator linked to D1R transmission, and found that horizontal, All amacrine, and some bipolar cells express this protein. To our knowledge, no studies have characterized D1R localization in bipolar cells since Veruki and Wässle (1996).

Wässle et al. (2009) established markers of bipolar cell types. In combination with bipolar cell type markers

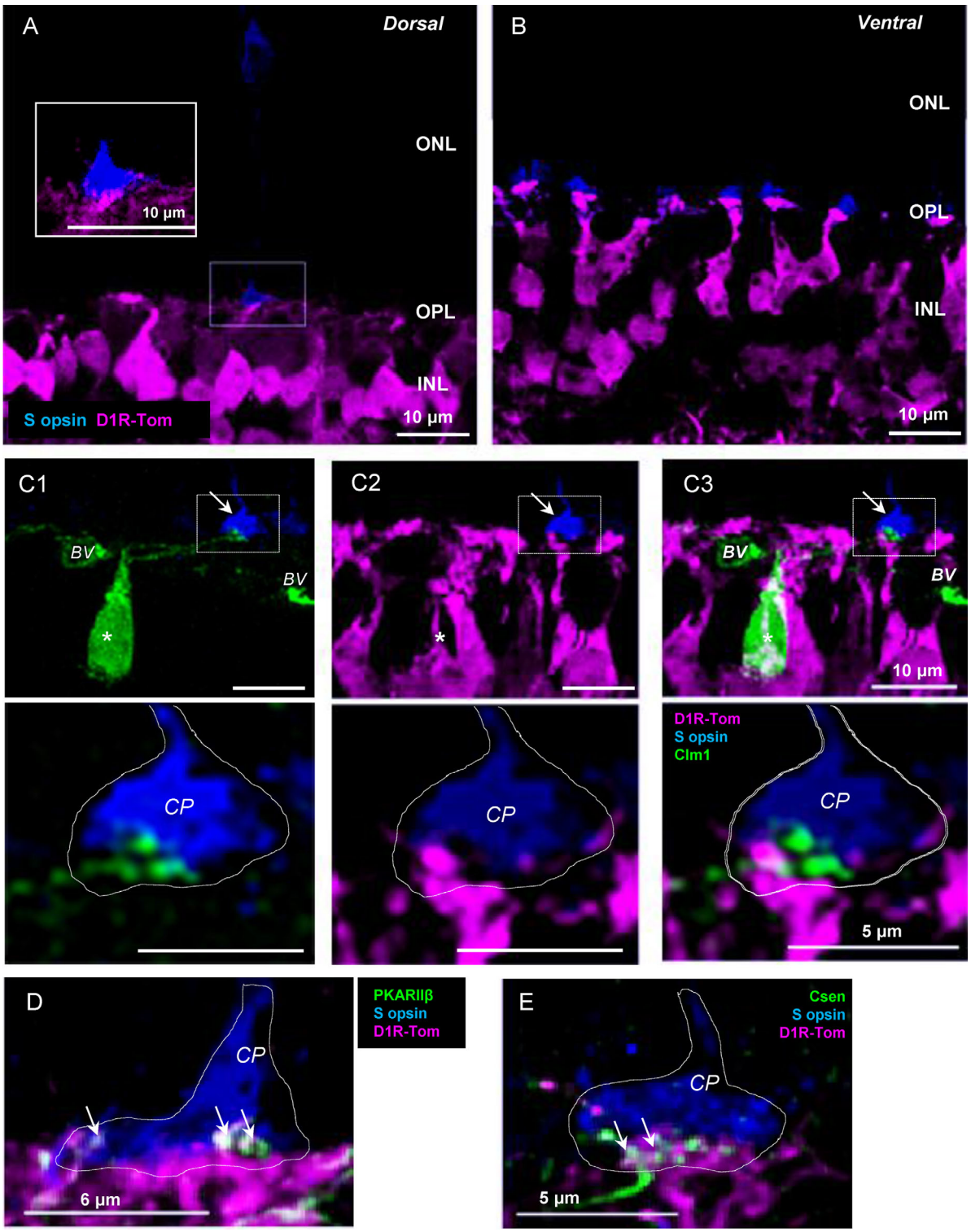

Figure 7. Genuine S-opsin-expressing cells and tdTomato processes. **A**: In the dorsal retina, S-cone terminals were occasionally observed, indicating that they were genuine S-cones. tdTomato fluorescent processes were attached to the terminal (see inset). **B**: In the ventral retina, S-opsin-expressing cells were frequently observed, indicating that they were mixed cones with S-opsin and M-opsin. **C1–C3**: Double transgenic mice with tdTomato and Clm-1 revealed that type 9 cells (*) did not express tdTomato. Type 9 and tdTomato positive processes associated with S-cone pedicle were not colocalized (arrow and magnified image seen in bottom row). **D**: tdTomato processes near S-cones expressed PKARIIβ which is a type 3b OFF bipolar cell marker. **E**: tdTomato processes attached to a genuine S-cone terminal were also partially colocalized with type 4 OFF bipolar cell dendrites (Csen). CP, cone pedicle; BV, blood vessel; CP, cone pedicle. Scale bars = 10 µm in C1-C3 upper and 5 µm in C1-C3 lower panels. [Color figure can be viewed in the online issue, which is available at wileyonlinelibrary.com.]

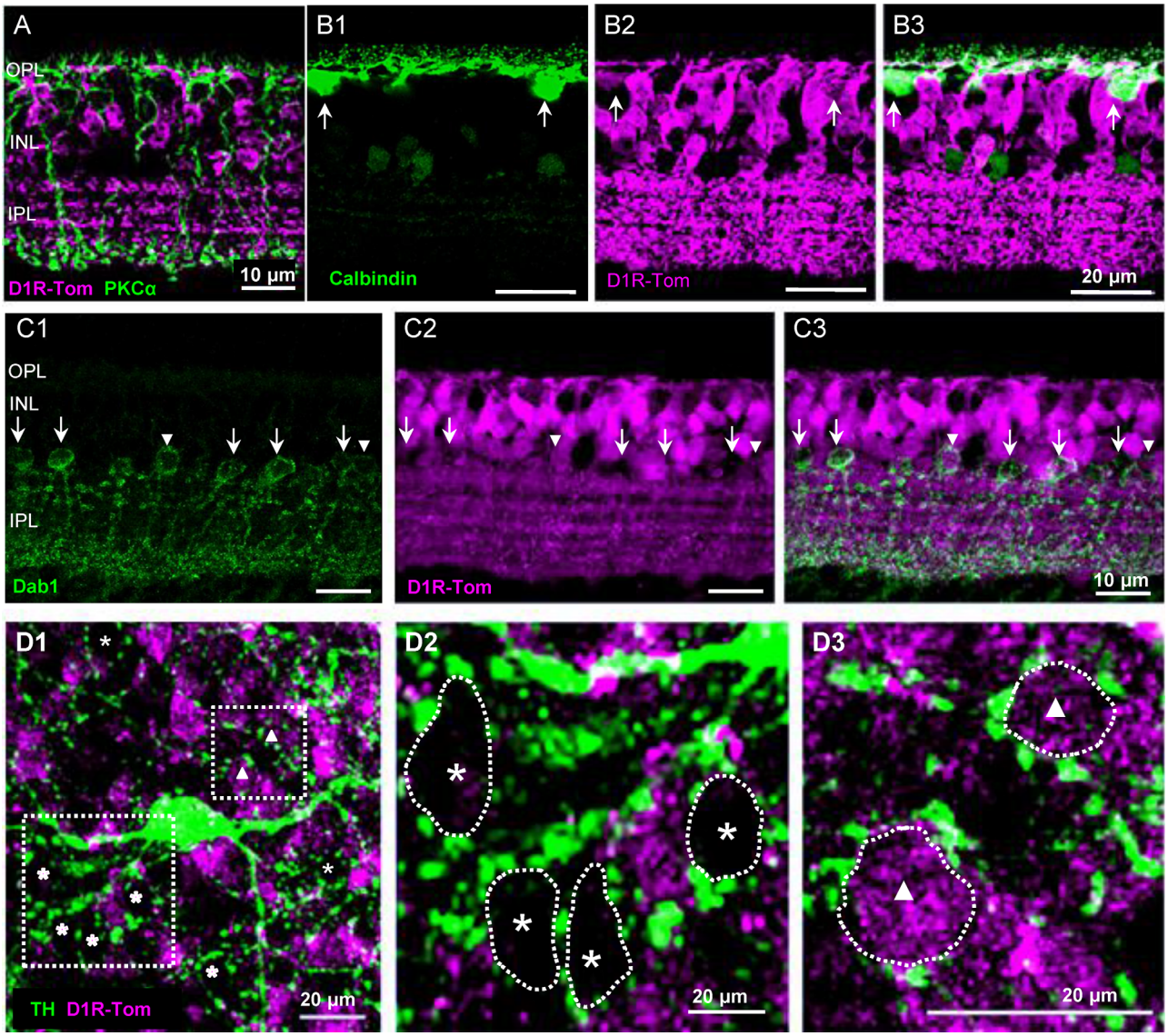

Figure 8. Rod bipolar cells, horizontal cells, and AII amacrine cells. **A**: Rod bipolar cells were labeled with PKCα, which did not colocalize with tdTomato. **B1–B3**: Calbindin-labeled horizontal cells colocalized with tdTomato (arrows). **C1–C3**: AII amacrine cells immunolabeled with disabled-1 (Dab-1) were not colocalized with tdTomato (arrows). ~25% Dab-1-positive cells were labeled with tdTomato (arrowheads). **D1**: In a flat-mount retinal preparation, TH staining revealed ring-like formations at the INL/ IPL border. **D2**: Most rings were not filled with tdTomato labeled cells (asterisk). (D3) ~25% of ring-like formations were filled with tdTomato-positive cells (triangle). Scale bars = 20 µm in B1-B3 and 10 µm in C1-C3. [Color figure can be viewed in the online issue, which is available at wileyonlinelibrary.com.]

and Drd1a-tdTomato transgenic mice, we investigated D1R expression in bipolar cells. OFF bipolar cell types were characterized using immunoreactive fluorescence markers. ON bipolar cell analysis was challenging because immunoreactive markers were only available for type 6. Therefore, we initially used an intracellular dye (neurobiotin)-injection technique to analyze type 5 and XBC bipolar cells (Fig. 4). Although we found that three type 5 cells were positive and two type 5 cells were negative for tdTomato expression, subset characterization was not conclusive only because of low efficiency of filling neurobiotin in type 5 cells. We therefore examined whether the HCN1 antibody can serve as a marker for a subset of type 5 ON bipolar cells. CtBP2 (ribbon synapse marker) colocalization analysis indicated that HCN1 is a type 5 cell marker (Fig. 5). We verified this with observation of bright HCN1 signaling, neurobiotin-injected XBCs, and type 5-2 cells colocalization (submitted). Using HCN1 immunoreactivity as a marker, we found that XBCs and type 5-2 cells colocalized with tdTomato, but another type 5-1 ON bipolar cells did not. Three different sets of type 5 cells were shown in the mouse retina (Helmstaedter et al., 2013; Ichinose et al., 2014). Among those, two

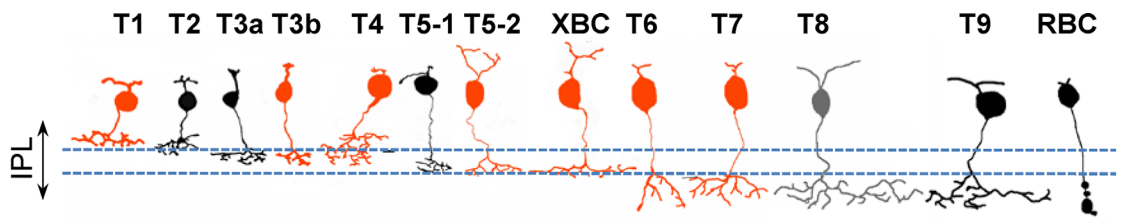

Subtype	1	2	3a	3b	4	5-1	5-2	XBC	6	7	8	9	RBC
Photoreceptor	Cone												Rod
Rod/cone inputs*	no	no	yes	yes	yes					yes (?)			
ON/OFF response	OFF					ON							
M- / S-opsin**	M	Mixed opsin input										S	
Transient/ sustained***	Sus	Tr.	Tr.	Sus	Sus	Sus	Tr.	Tr.	Tr.	Tr.	Sus	u.k	Sus
D1R expression	Yes	No	No	Yes	Yes	No	Yes	Yes	Yes	Yes	u.k	No	No

Figure 9. Summarized scheme showing Drd1a-tdTomato expression in each type of bipolar cell. Orange; tdTomato positive, type 1, 3b, 4, 5-2, XBC, 6, and 7 bipolar cells. Black; tdTomato negative, type 2, 3a, 5-1, 9, and rod bipolar cells, Gray: not studied, type 8. The table summarizes each type bipolar cell function. u.k.: unknown *Types receiving mixed rod and cone inputs (Mataruga et al., 2007; Tsukamoto et al., 2007; Haverkamp et al., 2008); **Chromatic characterization in each type (Breuninger et al., 2011; Ichinose et al., 2014); ***Temporal properties of each type (Euler and Masland, 2000; Ichinose et al., 2014; Ichinose and Hellmer, 2015). [Color figure can be viewed in the online issue, which is available at wileyonlinelibrary.com.]

sets of type 5 cells expressed D1Rs while another did not.

For analyzing type 7 and 9 bipolar cells, we generated double transgenic mice with Drd1a-tdTomato and Gus8.4-GFP (type 7) or Clomeleon 1 (type 9). Gus-GFP-positive type 7 bipolar cells clearly colocalized with tdTomato ($n = 91$ cells in 3 mice). In Clomeleon 1 double transgenic mice, all 15 type 9 cells were negative for tdTomato (4 mice). The small number of type 9 cells is likely attributable to the weaker bipolar cell staining over the Clm-YFP mice generations (personal communication with Dr. Silke Haverkamp).

Bipolar cell functions and dopamine

Maguire and Werblin (1994) demonstrated that glutamate puff-evoked responses in salamander OFF bipolar cells were increased by dopamine application, and this effect was mediated via D1Rs. Also, Wellis and Werblin (1995) recorded gamma-aminobutyric acid (GABA) puff-evoked inhibitory currents from bipolar cells, which were reduced by dopamine signaling through D1Rs. Both results demonstrate that dopamine modulates bipolar cell excitatory signaling. We found that D1Rs are expressed in a type-dependent manner, indicating that dopamine modulates visual processing pathways in the bipolar cell matrix. How does dopamine modulate bipolar cell visual signaling? The bipolar cell type-dependent properties are summarized in Figure 9, and the potential functions of dopamine in the bipolar cell network are discussed below.

D1Rs were expressed in cone bipolar cells but not in rod bipolar cells (Fig. 9), which is consistent with the fact that dopamine is released in mesopic to photopic conditions. However, a subset of cone bipolar cells receives mixed inputs both from cones and rods. If D1Rs are expressed in mixed rod/cone input bipolar cells, dopamine might play a role in switching from rod-dominant to cone-dominant signaling. Types 3a, 3b, 4, and 7 receive mixed inputs (Mataruga et al., 2007; Tsukamoto et al., 2007; Haverkamp et al., 2008) while types 1 and 2 receive inputs only from cones

(Haverkamp et al., 2006) (Fig. 9). Rod and cone mixed inputs types do not match D1R-expressing bipolar cell types, and thus, D1R signaling might not play a role in changing the dominancy of rod- and cone-inputs.

Two bipolar cell types are designated color-coded cells. Type 9 cells are S-cone-selective blue ON bipolar cells, whereas type 1 cells are M-opsin-selective green OFF bipolar cells (Fig. 9). All other bipolar cells receive inputs both from S-cones and M-cones (Breuninger et al., 2011; Ichinose et al., 2014). D1R-expressing bipolar cell types do not match chromatic pathways; thus, dopamine may not have a major role in color vision.

Similarly, dopamine might not play a role in gap junction regulation in bipolar cells. Gap junctions are electrical synapses that are dynamically regulated by illumination. Although ON cone bipolar cells make gap junction connections with AII amacrine cells, nitric oxide appears to be the key regulator rather than dopamine (Mills and Massey, 1995).

AII–AII coupling is regulated both by dopamine and ON bipolar cell activity through postsynaptic N-methyl-D-aspartate (NMDA) receptors (Kothmann et al., 2009, 2012). Our results showed that 25% of AII amacrine cells express D1Rs, while others do not express D1Rs (Fig. 8C,D). This might indicate that there are multiple regulation systems of AII–AII couplings.

Ichinose and Lukasiewicz (2007) demonstrated that dopamine reduces the voltage-gated Na^+ current, resulting in reduced light-evoked responses in a subset of bipolar cells in the salamander retina. This is consistent with observations in the mammalian retina using electroretinogram (ERG) analysis (Mojumder et al., 2008; Smith et al., 2014). Voltage-gated channel activity is regulated by G-protein-coupled receptor (GPCR)-mediated phosphorylation, which can be a target of dopamine modulation (Surmeier et al., 1992; Cantrell et al., 1997; Catterall, 2000; Cantrell and Catterall, 2001). Voltage-gated channels are heterogeneously expressed among bipolar cells (Connaughton and Maguire, 1998; Pan, 2000; Puthussery et al., 2013). Although we do not currently know which types of bipolar cells possess GPCR-regulated voltage-gated channels, this may be the target of dopamine for modulating bipolar cell visual signaling. Because the time course of voltage-gated channel activation is tightly regulated by its own channel properties, channel activity might modulate time-domain of visual processing, temporal processing.

Detailed maps of temporal tuning in bipolar cells have been described by several groups (Baden et al., 2013; Borghuis et al., 2013; Ichinose et al., 2014). Bipolar cell light responses are roughly divided into two types: transient and sustained responses to step-light stimuli reflection of high and low temporal tuning, respectively (Awatramani and Slaughter, 2000; Euler and Masland, 2000; Ichinose et al., 2005). Figure 9 integrates the findings of the present study with previous results from our laboratory (Ichinose et al., 2014; Ichinose and Hellmer, 2015). This summary highlights the significance of understanding D1R distribution across the different types of bipolar cells as related to transient versus sustained response to step-light stimulation. With the inclusion of the D1R expression data, we may have found a correlation between temporal properties and D1R expression. In ON bipolar cells, D1Rs are expressed in transient but not sustained cells. Conversely, D1Rs are expressed in sustained but not transient OFF bipolar cells. These results strongly suggest that D1R signaling in bipolar cells plays a role in temporal processing. Consistent with this notion, patients with Parkinson's disease exhibit a deficit in flicker sensitivity, which might be attributable to dysfunctional transiently responding cells (Djamgoz et al., 1997; Jackson and Owsley, 2003).

In summary, our results provide evidence for a more complex D1R localization within the bipolar cell network of the mouse retina than previously realized, suggesting more important modulatory roles for dopamine in the sculpting of visual signaling pathways. This suggests that dopamine supports and strengthens multiple cone-mediated and motion and/or flicker-sensitive pathways.

ACKNOWLEDGMENTS

We thank G. Kapatos (Wayne State University) for generously providing the Drd1a-tdTomato mice and the TH antibody, R.F. Margolskee for the gift of GUS8.4-GFP mice, D.-Q. Zhang for the gift of dab-1 antibody, and A.A. Hirano for her gift of the NK3R antibody. We also thank R. Barret and K. Vistisen of the Vision Core Facility for their experimental support and N. Challa for neurobiotin injection support. We also thank Drs. Z.-H. Pan, D.-Q. Zhang, and P.D. Lukasiewicz for insightful comments on the article.

CONFLICT OF INTEREST

The authors declare no competing financial interests.

ROLE OF AUTHORS

All authors had full access to all the data in the study and take responsibility for the integrity of the data and the accuracy of the data analysis. Study concept and design: PDW and TI. Acquisition of data: PF, BF, DMK, and TI. Analysis and interpretation of data: PF, BF, PDW, and TI. Drafting of the article: TI. Critical revision of the article for important intellectual content: PF, BF, DMK, PDW and TI. Statistical analysis: PDW and

TI. Obtained funding: PDW and TI. Technical support: PF, BF, DMK, and TI. PF and BF equally contributed.

LITERATURE CITED

Ade KK, Wan Y, Chen M, Gloss B, Calakos N. 2011. An Improved BAC transgenic fluorescent reporter line for sensitive and specific identification of striatonigral medium spiny neurons. Front Syst Neurosci 5:32.

Awatramani GB, Slaughter MM. 2000. Origin of transient and sustained responses in ganglion cells of the retina. J Neurosci 20:7087–7095.

Baden T, Berens P, Bethge M, Euler T. 2013. Spikes in mammalian bipolar cells support temporal layering of the inner retina. Curr Biol 23:48–52.

Bloomfield SA, Volgyi B. 2009. The diverse functional roles and regulation of neuronal gap junctions in the retina. Nat Rev Neurosci 10:495–506.

Borghuis BG, Marvin JS, Looger LL, Demb JB. 2013. Two-photon imaging of nonlinear glutamate release dynamics at bipolar cell synapses in the mouse retina. J Neurosci 33: 10972–10985.

Breuninger T, Puller C, Haverkamp S, Euler T. 2011. Chromatic bipolar cell pathways in the mouse retina. J Neurosci 31:6504–6517.

Caille I, Dumartin B, Bloch B. 1996. Ultrastructural localization of D1 dopamine receptor immunoreactivity in rat striatonigral neurons and its relation with dopaminergic innervation. Brain Res 730:17–31.

Cangiano L, Gargini C, Della Santina L, Demontis GC, Cervetto L. 2007. High-pass filtering of input signals by the Ih current in a non-spiking neuron, the retinal rod bipolar cell. PLoS ONE 2:e1327.

Cantrell AR, Catterall WA. 2001. Neuromodulation of Na + -channels: an unexpected form of cellular plasticity. Nat Rev Neurosci 2:397–407.

Cantrell AR, Smith RD, Goldin AL, Scheuer T, Catterall WA. 1997. Dopaminergic modulation of sodium current in hippocampal neurons via cAMP-dependent phosphorylation of specific sites in the sodium channel alpha subunit. J Neurosci 17:7330–7338.

Catterall WA. 2000. Structure and regulation of voltage-gated Ca2 + channels. Annu Rev Cell Dev Biol 16:521–555.

Cohen AI, Todd RD, Harmon S, O'Malley KL. 1992. Photoreceptors of mouse retinas possess D4 receptors coupled to adenylate cyclase. Proc Natl Acad Sci U S A 89: 12093–12097.

Connaughton VP, Maguire G. 1998. Differential expression of voltage-gated K + and Ca2 + currents in bipolar cells in the zebrafish retinal slice. Eur J Neurosci 10:1350–1362.

Contini M, Lin B, Kobayashi K, Okano H, Masland RH, Raviola E. 2010. Synaptic input of ON-bipolar cells onto the dopaminergic neurons of the mouse retina. J Comp Neurol 518:2035–2050.

Deans MR, Volgyi B, Goodenough DA, Bloomfield SA, Paul DL. 2002. Connexin36 is essential for transmission of rod-mediated visual signals in the mammalian retina. Neuron 36:703–712.

Deng YP, Lei WL, Reiner A. 2006. Differential perikaryal localization in rats of D1 and D2 dopamine receptors on striatal projection neuron types identified by retrograde labeling. J Chem Neuroanat 32:101–116.

Djamgoz MB, Hankins MW, Hirano J, Archer SN. 1997. Neurobiology of retinal dopamine in relation to degenerative states of the tissue. Vision Res 37:3509–3529.

Dong CJ, McReynolds JS. 1991. The relationship between light, dopamine release and horizontal cell coupling in the mudpuppy retina. J Physiol 440:291–309.

Dumitrescu ON, Pucci FG, Wong KY, Berson DM. 2009. Ectopic retinal ON bipolar cell synapses in the OFF inner plexiform layer: contacts with dopaminergic amacrine cells and melanopsin ganglion cells. J Comp Neurol 517:226–244.

Euler T, Masland RH. 2000. Light-evoked responses of bipolar cells in a mammalian retina. J Neurophysiol 83:1817–1829.

Euler T, Haverkamp S, Schubert T, Baden T. 2014. Retinal bipolar cells: elementary building blocks of vision. Nat Rev Neurosci 15:507–519.

Fyk-Kolodziej B, Pourcho RG. 2007. Differential distribution of hyperpolarization-activated and cyclic nucleotide-gated channels in cone bipolar cells of the rat retina. J Comp Neurol 501:891–903.

Ghosh KK, Bujan S, Haverkamp S, Feigenspan A, Wässle H. 2004. Types of bipolar cells in the mouse retina. J Comp Neurol 469:70–82.

Hampson EC, Vaney DI, Weiler R. 1992. Dopaminergic modulation of gap junction permeability between amacrine cells in mammalian retina. J Neurosci 12:4911–4922.

Hampson EC, Weiler R, Vaney DI. 1994. pH-gated dopaminergic modulation of horizontal cell gap junctions in mammalian retina. Proc Biol Sci 255:67–72.

Haverkamp S, Wässle H, Duebel J, Kuner T, Augustine GJ, Feng G, Euler T. 2005. The primordial, blue-cone color system of the mouse retina. J Neurosci 25:5438–5445.

Haverkamp S, Michalakis S, Claes E, Seeliger MW, Humphries P, Biel M, Feigenspan A. 2006. Synaptic plasticity in CNGA3(-/-) mice: cone bipolar cells react on the missing cone input and form ectopic synapses with rods. J Neurosci 26:5248–5255.

Haverkamp S, Specht D, Majumdar S, Zaidi NF, Brandstatter JH, Wasco W, Wässle H, Tom Dieck S. 2008. Type 4 OFF cone bipolar cells of the mouse retina express calsenilin and contact cones as well as rods. J Comp Neurol 507: 1087–1101.

Helmstaedter M, Briggman KL, Turaga SC, Jain V, Seung HS, Denk W. 2013. Connectomic reconstruction of the inner plexiform layer in the mouse retina. Nature 500:168–174.

Huang L, Shanker YG, Dubauskaite J, Zheng JZ, Yan W, Rosenzweig S, Spielman AI, Max M, Margolskee RF. 1999. Ggamma13 colocalizes with gustducin in taste receptor cells and mediates IP3 responses to bitter denatonium. Nat Neurosci 2:1055–1062.

Huang L, Max M, Margolskee RF, Su H, Masland RH, Euler T. 2003. G protein subunit G gamma 13 is coexpressed with G alpha o, G beta 3, and G beta 4 in retinal ON bipolar cells. J Comp Neurol 455:1–10.

Ichinose T, Hellmer CB. 2015. Differential signaling and glutamate receptor compositions in the OFF bipolar cell types in the mouse retina. J Physiol [Epub ahead of print].

Ichinose T, Lukasiewicz PD. 2007. Ambient light regulates sodium channel activity to dynamically control retinal signaling. J Neurosci 27:4756–4764.

Ichinose T, Shields CR, Lukasiewicz PD. 2005. Sodium channels in transient retinal bipolar cells enhance visual responses in ganglion cells. J Neurosci 25:1856–1865.

Ichinose T, Fyk-Kolodziej B, Cohn J. 2014. Roles of ON cone bipolar cell subtypes in temporal coding in the mouse retina. J Neurosci 34:8761–8771.

Jackson GR, Owsley C. 2003. Visual dysfunction, neurodegenerative diseases, and aging. Neurol Clin 21:709–728.

Jarvie KR, Booth G, Brown EM, Niznik HB. 1989. Glycoprotein nature of dopamine D1 receptors in the brain and parathyroid gland. Mol Pharmacol 36:566–574.

Jin NG, Chuang AZ, Masson PJ, Ribelayga CP. 2015. Rod electrical coupling is controlled by a circadian clock and dopamine in mouse retina. J Physiol 593:1597–1631.

Kindler S, Wang H, Richter D, Tiedge H. 2005. RNA transport and local control of translation. Annu Rev Cell Dev Biol 21:223–245.

Kothmann WW, Massey SC, O'Brien J. 2009. Dopamine-stimulated dephosphorylation of connexin 36 mediates AII amacrine cell uncoupling. J Neurosci 29:14903–14911.

Kothmann WW, Trexler EB, Whitaker CM, Li W, Massey SC, O'Brien J. 2012. Nonsynaptic NMDA receptors mediate activity-dependent plasticity of gap junctional coupling in the AII amacrine cell network. J Neurosci 32:6747–6759.

Luedtke RR, Griffin SA, Conroy SS, Jin X, Pinto A, Sesack SR. 1999. Immunoblot and immunohistochemical comparison of murine monoclonal antibodies specific for the rat D1a and D1b dopamine receptor subtypes. J Neuroimmunol 101:170–187.

Maguire G, Werblin F. 1994. Dopamine enhances a glutamate-gated ionic current in OFF bipolar cells of the tiger salamander retina. J Neurosci 14:6094–6101.

Mangel SC, Dowling JE. 1985. Responsiveness and receptive field size of carp horizontal cells are reduced by prolonged darkness and dopamine. Science 229:1107–1109.

Mataruga A, Kremmer E, Muller F. 2007. Type 3a and type 3b OFF cone bipolar cells provide for the alternative rod pathway in the mouse retina. J Comp Neurol 502:1123–1137.

Mills SL, Massey SC. 1995. Differential properties of two gap junctional pathways made by AII amacrine cells. Nature 377:734–737.

Mojumder DK, Sherry DM, Frishman LJ. 2008. Contribution of voltage-gated sodium channels to the b-wave of the mammalian flash electroretinogram. J Physiol 586:2551–2580.

Mora-Ferrer C, Yazulla S, Studholme KM, Haak-Frendscho M. 1999. Dopamine D1-receptor immunolocalization in goldfish retina. J Comp Neurol 411:705–714.

Muller F, Scholten A, Ivanova E, Haverkamp S, Kremmer E, Kaupp UB. 2003. HCN channels are expressed differentially in retinal bipolar cells and concentrated at synaptic terminals. Eur J Neurosci 17:2084–2096.

Nguyen-Legros J, Simon A, Caille I, Bloch B. 1997. Immunocytochemical localization of dopamine D1 receptors in the retina of mammals. Vis Neurosci 14:545–551.

Ogata G, Stradleigh TW, Partida GJ, Ishida AT. 2012. Dopamine and full-field illumination activate D1 and D2-D5-type receptors in adult rat retinal ganglion cells. J Comp Neurol 520:4032–4049.

Pan ZH. 2000. Differential expression of high- and two types of low-voltage-activated calcium currents in rod and cone bipolar cells of the rat retina. J Neurophysiol 83:513–527.

Pignatelli V, Strettoi E. 2004. Bipolar cells of the mouse retina: a gene gun, morphological study. J Comp Neurol 476:254–266.

Puthussery T, Venkataramani S, Gayet-Primo J, Smith RG, Taylor WR. 2013. NaV1.1 channels in axon initial segments of bipolar cells augment input to magnocellular visual pathways in the primate retina. J Neurosci 33:16045–16059.

Ribelayga C, Cao Y, Mangel SC. 2008. The circadian clock in the retina controls rod-cone coupling. Neuron 59:790–801.

Rice DS, Curran T. 2000. Disabled-1 is expressed in type AII amacrine cells in the mouse retina. J Comp Neurol 424:327–338.

Shuen JA, Chen M, Gloss B, Calakos N. 2008. Drd1a-tdTomato BAC transgenic mice for simultaneous visualization of medium spiny neurons in the direct and indirect pathways of the basal ganglia. J Neurosci 28:2681–2685.

Smith BJ, Cote PD, Tremblay F. 2014. D1 Dopamine receptors modulate cone ON bipolar cell Nav channels to control daily rhythms in photopic vision. Chronobiol Int 1–11.

Soto F, Bleckert A, Lewis R, Kang Y, Kerschensteiner D, Craig AM, Wong RO. 2011. Coordinated increase in inhibitory and excitatory synapses onto retinal ganglion cells during development. Neural Dev 6:31.

Stella SL Jr, Thoreson WB. 2000. Differential modulation of rod and cone calcium currents in tiger salamander retina by D2 dopamine receptors and cAMP. Eur J Neurosci 12:3537–3548.

Surmeier DJ, Eberwine J, Wilson CJ, Cao Y, Stefani A, Kitai ST. 1992. Dopamine receptor subtypes colocalize in rat striatonigral neurons. Proc Natl Acad Sci U S A 89:10178–10182.

Szel A, Rohlich P, Caffe AR, Juliusson B, Aguirre G, Van Veen T. 1992. Unique topographic separation of two spectral classes of cones in the mouse retina. J Comp Neurol 325:327–342.

Thibault D, Loustalot F, Fortin GM, Bourque MJ, Trudeau LE. 2013. Evaluation of D1 and D2 dopamine receptor segregation in the developing striatum using BAC transgenic mice. PLoS ONE 8:e67219.

Ting JT, Feng G. 2014. Recombineering strategies for developing next generation BAC transgenic tools for optogenetics and beyond. Front Behav Neurosci 8:111.

tom Dieck S, Altrock WD, Kessels MM, Qualmann B, Regus H, Brauner D, Fejtova A, Bracko O, Gundelfinger ED, Brandstatter JH. 2005. Molecular dissection of the photoreceptor ribbon synapse: physical interaction of Bassoon and RIBEYE is essential for the assembly of the ribbon complex. J Cell Biol 168:825–836.

Tsukamoto Y, Morigiwa K, Ishii M, Takao M, Iwatsuki K, Nakanishi S, Fukuda Y. 2007. A novel connection between rods and ON cone bipolar cells revealed by ectopic metabotropic glutamate receptor 7 (mGluR7) in mGluR6-deficient mouse retinas. J Neurosci 27:6261–6267.

Urschel S, Hoher T, Schubert T, Alev C, Sohl G, Worsdorfer P, Asahara T, Dermietzel R, Weiler R, Willecke K. 2006. Protein kinase A-mediated phosphorylation of connexin36 in mouse retina results in decreased gap junctional communication between AII amacrine cells. J Biol Chem 281:33163–33171.

Van Hook MJ, Wong KY, Berson DM. 2012. Dopaminergic modulation of ganglion-cell photoreceptors in rat. Eur J Neurosci 35:507–518.

Vaquero CF, Pignatelli A, Partida GJ, Ishida AT. 2001. A dopamine- and protein kinase A-dependent mechanism for network adaptation in retinal ganglion cells. J Neurosci 21:8624–8635.

Veruki ML, Wässle H. 1996. Immunohistochemical localization of dopamine D1 receptors in rat retina. Eur J Neurosci 8:2286–2297.

Voigt T, Wässle H. 1987. Dopaminergic innervation of A II amacrine cells in mammalian retina. J Neurosci 7:4115–4128.

Volgyi B, Debertin G, Balogh M, Popovich E, Kovacs-Oller T. 2014. Compartment-specific tyrosine hydroxylase-positive innervation to AII amacrine cells in the rabbit retina. Neuroscience 270:88–97.

Wässle H. 2004. Parallel processing in the mammalian retina. Nat Rev Neurosci 5:747–757.

Wässle H, Puller C, Muller F, Haverkamp S. 2009. Cone contacts, mosaics, and territories of bipolar cells in the mouse retina. J Neurosci 29:106–117.

Wellis DP, Werblin FS. 1995. Dopamine modulates GABAc receptors mediating inhibition of calcium entry into and transmitter release from bipolar cell terminals in tiger salamander retina. J Neurosci 15(7 Pt 1):4748–4761.

Witkovsky P. 2004. Dopamine and retinal function. Doc Ophthalmol 108:17–40.

Witkovsky P, Svenningsson P, Yan L, Bateup H, Silver R. 2007. Cellular localization and function of DARPP-32 in the rodent retina. Eur J Neurosci 25:3233–3242.

Xin D, Bloomfield SA. 1999. Dark- and light-induced changes in coupling between horizontal cells in mammalian retina. J Comp Neurol 405:75–87.

Zhang DQ, Zhou TR, McMahon DG. 2007. Functional heterogeneity of retinal dopaminergic neurons underlying their multiple roles in vision. J Neurosci 27:692–699.

Zinchuk V, Wu Y, Grossenbacher-Zinchuk O, Stefani E. 2011. Quantifying spatial correlations of fluorescent markers using enhanced background reduction with protein proximity index and correlation coefficient estimations. Nat Protoc 6:1554–1567.